





## Article

# Proof-of-Concept Study on the Feasibility of Supercritical Carbon Dioxide-Assisted Consolidation Treatment for a Pair of Goalkeeper Gloves on Synthetic Latex-Based Foam Mock-Ups

Joana Tomás Ferreira <sup>1</sup>, Angelica Bartoletti <sup>1,2,\*</sup>, Susana França de Sá <sup>1</sup>, Anita Quye <sup>3</sup>, Yvonne Shashoua <sup>4</sup>, Teresa Casimiro <sup>5</sup> and Joana Lia Ferreira <sup>6,\*</sup>

- <sup>1</sup> LAQV-REQUIMTE and Department of Conservation and Restoration, NOVA School of Science and Technology, Universidade NOVA de Lisboa, 2829-516 Caparica, Portugal; jt.ferreira@campus.fct.unl.pt (J.T.F.)
- <sup>2</sup> Conservation Department, Tate Britain, Millbank, London SW1P 4RG, UK
- <sup>3</sup> Kelvin Centre for Conservation and Cultural Heritage Research, School of Culture and Creative Arts, University of Glasgow, Glasgow G12 8QH, UK; anita.quye@glasgow.ac.uk
- <sup>4</sup> Environmental Archaeology and Materials Science, National Museum of Denmark, 2800 Kongens Lyngby, Denmark; ysh@natmus.dk
- <sup>5</sup> LAQV-REQUIMTE and Department of Chemistry, NOVA School of Science and Technology, Universidade NOVA de Lisboa, 2829-516 Caparica, Portugal; teresa.casimiro@fct.unl.pt
- <sup>6</sup> CIUHCT—Interuniversity Center for the History of Sciences and Technology and Department of Conservation and Restoration, NOVA School of Science and Technology, Universidade NOVA de Lisboa, 2829-516 Caparica, Portugal
- \* Correspondence: angelica.bartoletti@tate.org.uk (A.B.); jlaf@fct.unl.pt (J.L.F.)

**Abstract:** This work investigates the suitability of supercritical fluid technology for designing a safe, efficient and sustainable consolidation treatment for a pair of heavily degraded goalkeeper gloves. Traditional methods have revealed themselves as unsafe and inefficient, leading to material loss and a minimal enhancement of surface cohesion. To overcome these limitations, the use of supercritical carbon dioxide (scCO<sub>2</sub>) was explored in a treatment, where scCO<sub>2</sub> behaves as a green solvent and consolidant carrier. In-depth and homogeneous application of the consolidant, without the need for direct contact with the foam material, was sought. As a proof of concept, the procedure was tested on samples that mimic the synthetic latex-based foam composition and condition of the object. Poly(vinyl acetate) was selected as a consolidant because its behaviour and solubility in scCO<sub>2</sub> are known. Several experimental conditions were explored to assess the impact and feasibility of the scCO<sub>2</sub>-assisted consolidation procedure. Empirical observations, optical microscopy, scanning electron microscopy and infrared spectroscopy were used to monitor potential modifications in the samples and assess the treatment efficacy. The results highlighted the advantages and pitfalls of scCO<sub>2</sub>-assisted consolidation, paving the way for fine-tuning the process. It neither damaged the fragile surfaces of the foam samples nor increased material loss, which is an advantage compared to traditional treatments. The performed analysis suggested that homogeneous impregnation of the foams was achieved. This study might be a turning point in the conservation of foam-based museum objects, as the results indicate the suitability of the scCO<sub>2</sub>-assisted consolidation process as a non-toxic and more efficient alternative, being safer for the object.

**Keywords:** supercritical CO<sub>2</sub>; impregnation; poly(vinyl acetate); sustainable conservation; cultural heritage; modern and contemporary materials; synthetic polymer materials; historical plastic objects



**Citation:** Tomás Ferreira, J.; Bartoletti, A.; França de Sá, S.; Quye, A.; Shashoua, Y.; Casimiro, T.; Ferreira, J.L. Proof-of-Concept Study on the Feasibility of Supercritical Carbon Dioxide-Assisted Consolidation Treatment for a Pair of Goalkeeper Gloves on Synthetic Latex-Based Foam Mock-Ups. *Sustainability* **2024**, *16*, 1562. <https://doi.org/10.3390/su16041562>

Academic Editor: Mariateresa Lettieri

Received: 9 January 2024

Revised: 7 February 2024

Accepted: 8 February 2024

Published: 13 February 2024



**Copyright:** © 2024 by the authors. Licensee MDPI, Basel, Switzerland. This article is an open access article distributed under the terms and conditions of the Creative Commons Attribution (CC BY) license (<https://creativecommons.org/licenses/by/4.0/>).

## 1. Introduction

The conservation of modern and contemporary artworks or design objects can prove challenging with respect to interventive conservation treatments, due to their inherent chemical-physical properties and the fact that plastics meant for everyday use have an intended shorter service life than other materials in museum collections. Research efforts

have focused on finding solutions for the most common and most unstable plastics encountered in museums, but there is still a lack of knowledge and strategic conservation plans for many other synthetic materials. Increasingly, plastic objects created for daily life activities and used by celebrities have achieved iconic status and historical value and have found their way into museums and collections, such as sports memorabilia [1–3].

These items are usually complex systems and highly challenging for the establishment of conservation strategies, as they are generally made of a combination of materials for which limited information on degradation pathways is available. In addition, they are often found in a post-use, worn condition with compromised physical integrity as a cumulative result of natural degradation and extensive use, jeopardising their legacy to future generations.

An example of such a complex case study is represented by a pair of goalkeeper gloves in the collection of Museu Benfica–Cosme Damião (Lisbon, Portugal) (Figure 1). The gloves were used by the professional football player Robert Enke, and the player's signature and handwritten dedication are visible on both palms (Figure 1b).



**Figure 1.** General views of Robert Enke's goalkeeper gloves (ca. 2000), currently part of Museu Benfica–Cosme Damião's collection. © Sport Lisboa e Benfica: (a) back and (b) palm section.

An interventive conservation treatment of this foam was considered urgent to minimise further loss or damage to the gloves, namely, the stabilisation of the top foam layer of the palms where the signature and dedications are, and its adhesion to the underneath layer. The treatment, however, proved to be particularly challenging due to the extensive degradation of the palm and its complex composition. Visual and molecular analysis of the material in previous studies [2,3] showed that it comprised a dense, semi-rigid foam with an open-cell structure and pores of varying sizes, based on synthetic latex, namely a blend of polyisoprene, polybutadiene and polystyrene, with the last two possibly as a copolymer.

While consolidation options for polyurethane (ether- and ester-based) foams have been the focus of some studies [4–9], there is currently no published research into appropriate consolidants and treatment methodologies for synthetic latex-based foams in the conservation literature. Consolidants are generally applied via direct methods like brushing or facing (brushing through a separating membrane), or indirect methods such as nebulisation or spraying. These procedures, however, have a series of drawbacks: the former has the risk of disrupting the surface and promoting detachment or loss, which would compromise the signatures and handwritten dedications on the palms, and the latter enables only a shallow penetration of the consolidant into the material, which would not inhibit the crumbling phenomena.

Despite recent efforts to find suitable procedures for the in-depth and safe penetration of consolidants, such as the study of low vacuum pressure to treat shoe soles made of closed-cell ester-based polyurethane (PUR) [10], an entirely satisfactory treatment has not yet been found. In addition, established consolidants used in conservation involve potentially

irritant or toxic materials that require appropriate health and safety requirements and PPE, such as the mixture of Impranal<sup>®</sup> DLV/1 (Covestro AG, Leverkusen, Germany) with Tinuvin B75 (BASF, Ludwigshafen, Germany) or hexamethyldisilane (HMDS) for ether- and ester-based PUR foams consolidation, respectively [4–7,9].

To explore appropriate conservation strategies for the goalkeeper gloves, initial tests were performed using currently available, aqueous dispersion-based consolidants (Impranal<sup>®</sup> DLV/1, Evacon-R<sup>™</sup> (CXD - Conservation by Design, Milton Keynes, UK), Plectol B500 (Synthomer, London, UK), Mowilith<sup>®</sup> LDM 7667 and Mowilith<sup>®</sup> LDM 1871 (Celanese Corporation, Texas, USA)), applied through nebulisation and facing techniques [3]. Among the tested consolidants, Evacon-R<sup>™</sup> and Mowilith<sup>®</sup> LDM 1871 performed best but could only guarantee a minimal enhancement of the surface cohesion. As expected, neither of the application procedures (nebulisation and facing) were suitable for the case study. Additionally, although consolidants applied via facing generally resulted in a deeper and more uniform penetration than spraying or nebulisation, their migration into the foam mock-ups remained superficial [3].

In the absence of safe and low-risk conservation procedures among those traditionally used by conservators [3], options used in other fields were evaluated. In industrial research, the difficulties and limitations of incorporating compounds into a matrix, such as the use of high temperatures, organic solvents, limited penetration depth, etc., can be overcome by using supercritical fluid technology [11].

A supercritical fluid is a highly compressible gas that, above a specific temperature and pressure values, the so-called critical temperature,  $T_c$ , and critical pressure,  $p_c$  (also known as critical point), simultaneously behaves like and exhibits physicochemical properties of a gas and a liquid. In common with a gas, it has low viscosity, high diffusivity and lack of surface tension. As a liquid, it has high density and solvation power [12–15]. These properties can be easily tuned by varying the temperature and pressure conditions of the system.

Carbon dioxide ( $\text{CO}_2$ ) has a relatively accessible critical point ( $T_c = 31\text{ }^\circ\text{C}$  and  $p_c = 7.38\text{ MPa}$ ) compared with other supercritical fluids and, for this reason, is most frequently selected for various industrial applications [12–14,16]. In addition, it is considered a green solvent because it is non-flammable, non-toxic, and relatively chemically inert. It is available in large quantities and high purity as a by-product of many industrial processes and can be readily recycled and reused [17–19].

The working principle of the  $\text{scCO}_2$ -assisted impregnation is based on the previously described versatile properties of fluids in supercritical conditions in which  $\text{CO}_2$  has a double function: it behaves as a solvent due to its high density and as a carrier, thanks to its high diffusion rate and lack of interfacial tension, which enables an easy in-depth and homogeneous penetration in a wide range of materials with minimal interaction. The procedure is performed in a high-pressure apparatus where the temperature and pressure are increased to achieve the supercritical conditions. At the end of the experiment, by returning to atmospheric pressure and temperature,  $\text{CO}_2$  can be easily released as a gas without leaving residues in the material [20].

Several variables can contribute to a successful impregnation: high solubility of the compound to impregnate in  $\text{scCO}_2$ ; affinity of the compound solution with the matrix, optimal temperature and pressure, and exposure and depressurisation times. Supercritical  $\text{CO}_2$  is a suitable solvent for nonpolar, very slightly polar and low molecular weight (MW) compounds [21–25], whilst it is a poor one for hydrophilic, polar molecules or compounds that have a MW above 1000 (such as polymers, proteins, aliphatic fatty acids, etc.) [21,22,25]. However, this does not apply to all polymers, as some are known to be soluble in  $\text{scCO}_2$ , even with high MW, such as the case of poly(vinyl acetate) [19,21,26,27]. In addition,  $\text{scCO}_2$  solvation power can be tuned either by adjusting temperature and pressure, which will impact its density and diffusivity, or by adding entrainers (i.e., co-solvents, surfactants, etc.) to increase or decrease its polarity, such as ethanol or methanol [13]. Exposure and depressurisation times can also be adjusted for better impregnation results. Exposure

should be sufficiently long to allow the transport and penetration of the compound into the material to be impregnated, while depressurisation time needs to be adjusted to minimise swelling and consequent deformation of the matrix under treatment (shorter times) or the complete removal of the impregnated compound during the exit of the CO<sub>2</sub> from the cell (longer times).

Examples of scCO<sub>2</sub>-assisted impregnation include the impregnation process for the dyeing of synthetic and natural textiles [28,29], preparation of drug-eluting implants [30–37], softwood processing [38–43], the preparation of hybrid silk material [44] or for food packaging applications [45,46]. In the conservation field, supercritical CO<sub>2</sub> technology is still niche, with a few examples of application such as the cleaning of textiles [47–51], deacidification of paper [52–56] and the removal of pesticides from objects in ethnographic collections [57–59]. However, there are no examples of consolidation treatments (the equivalent to impregnation as a conservation treatment), except for a study by Tuminello et al. on the solubility of fluorinated resins in liquid CO<sub>2</sub> and their application via CO<sub>2</sub> spraying for stone preservation [60]. The use of scCO<sub>2</sub> is also relatively unexplored in treating plastics of historical value [61,62], with no previous investigation of application on synthetic latex-based foam materials or even in more frequently found types of foams, such as polyurethane (PUR).

#### *Aim and Viability of the Research*

The present study aimed to assess the impact of scCO<sub>2</sub> on a synthetic latex-based foam composed of a blend of polyisoprene, polybutadiene and polystyrene (the last two possibly as a copolymer) and the feasibility of the scCO<sub>2</sub>-assisted consolidation process for this material, which was tested on mock-ups representing the goalkeeper gloves case study, prepared using modern equivalent materials and selected based on previous research [2,3]. The scCO<sub>2</sub>-assisted consolidation was investigated as an alternative method to the traditional consolidation procedures previously tested for the treatment of the same case study, namely brushing and nebulisation [3]. In particular, it aimed to overcome the limitations of the need for direct contact with the material, which can potentially lead to material losses, while still achieving an in-depth and homogeneous deposition of the consolidant.

As mentioned above, polymers exhibit very low solubility in CO<sub>2</sub>, including those found in the gloves [21,23,26]; hence, it is expected that scCO<sub>2</sub> will not affect the synthetic latex-based foam. However, published studies have focused on unaged polymers [21,23,26], and the solubility of a polymer in CO<sub>2</sub> might alter with deterioration, particularly considering that the presence of an interaction site such as a carbonyl group (which is present in degradation products) is known to improve its solubility in CO<sub>2</sub> [22,23,63,64]. Moreover, sorption of CO<sub>2</sub> by the polymer might occur, with consequent swelling, potential variations in mechanical properties and a decrease in the glass transition temperature (T<sub>g</sub>) [65–68].

To test the viability of the scCO<sub>2</sub>-assisted consolidation for this particular case study, and in general, for foam-based materials, poly(vinyl acetate) (PVAc) was selected as a consolidant, because its solubility and behaviour in scCO<sub>2</sub> are known, even with a high MW [21,22,26,27,69]. In addition, vinyl acetate is the component with adhesive properties in the aqueous copolymer dispersions Evacon-R™ and Mowilith® LDM 1871, which provided the best results in previous consolidation tests for this foam material [3]. Previous studies have also shown its good stability towards ageing when used as a homopolymer [70,71].

Extensive trials were performed on mock-up samples prepared using modern equivalents for the aged historical material of the gloves. A multi-analytical characterisation approach, comprising empirical observation, colour measurements, imaging with stereomicroscopy, optical microscopy (OM) and scanning electron microscopy (SEM), and attenuated total reflection Fourier transform infrared spectroscopy (ATR-FTIR) was used to monitor physical and chemical changes in the samples and the effect of consolidation.

## 2. Materials and Methods

### 2.1. Mock-Up Sample Preparation

Mock-up samples were prepared using modern equivalent materials to the case study. Goalkeeper gloves from Nike (model Nike GK Match, Nike, Beaverton, OR, USA) were selected based on their similarity in appearance, structure and composition with the original materials of the gloves, as discussed elsewhere [2,3]. To simulate the degradation conditions of the original pair of gloves, the test gloves were first used, to introduce some deterioration due to mechanical wear and to transfer some natural perspiration, which was considered a crucial agent in the ageing of the original gloves and was covered elsewhere [2,3]. Ageing with polychromatic irradiation was carried out in a light chamber (Solarbox 3000e, CO.FO.ME.GRA, Milan, Italy) equipped with a Xenon-arc light source and an outdoor filter ( $\lambda \geq 280$  nm, CO.FO.ME.GRA, Milan, Italy) with constant irradiation of  $800 \text{ W/m}^2$ . The temperature inside the apparatus was stable at approximately  $40 \text{ }^\circ\text{C}$ . Samples were irradiated for six days, then transferred to a climatic chamber and heated at  $60 \text{ }^\circ\text{C}$  and 75% of relative humidity for twelve additional days. After finalising accelerated ageing, the back and the palm sections were separated, and small pieces of approximately  $10 \times 15 \times 5$  mm were cut from the latter and used for  $\text{scCO}_2$  trials.

### 2.2. Materials

Poly(vinyl acetate) (PVAc) with molecular weights (MW) of approximately 83,000 and 167,000 in the form of beads, and ethanol (EtOH, assay  $\geq 99.8\%$ ) were purchased from Sigma-Aldrich (St. Louis, MO, USA). The PVAc beads were ground finely to reduce particle size and facilitate their solubilisation in  $\text{scCO}_2$ . Carbon dioxide (purity 99.998%) was purchased from Air Liquide (Paris, France).

### 2.3. Carbon Dioxide ( $\text{CO}_2$ ) Apparatus, Experimental Conditions and Procedure

As previously stated, the use of  $\text{scCO}_2$  is relatively unexplored in treating plastics of historical value [61,62], with no previous research of application on foams, including synthetic latex-based or the more frequently common PUR ones. Hence, initial tests were performed to assess the safety of the method for the foam samples, i.e., the impact of the  $\text{scCO}_2$  and the selected experimental conditions on the samples, and to evaluate potential induced changes, such as visual, morphological or molecular alterations.

These initial trials were performed in low- and high-pressure conditions with different pressurisation, exposure and depressurisation times to assess the safety of the method at these conditions for the foams. Test 1 (Table 1) was conducted at milder conditions with temperature and pressure values of  $33 \text{ }^\circ\text{C}$  and 10 MPa. Up to a pressure of approximately 30 MPa, it was possible to use the high-pressure cell with a sapphire window at each end, which enabled visual access to the samples during the experiment. To monitor the response of the samples to variations in pressure and avoid inducing damage, the desired pressure was reached by a slow pressurisation over 40 min; samples remained at the selected experimental conditions for 30 min and were brought back to atmospheric values through a very slow depressurisation (120 min). By contrast, Test 2 (Table 1) was performed at more extreme conditions: a pressure of 36 MPa, which required the substitution of the sapphire windows for stainless-steel ones with no visual access to the interior of the cell, faster pressurisation and depressurisation times (10 and 5 min, respectively) and a longer exposure time (120 min). The temperature was also slightly increased to  $40 \text{ }^\circ\text{C}$ . Higher temperature values were not considered to avoid inducing thermal degradation to specimens.

**Table 1.** Summary of experimental conditions used for testing the safety of CO<sub>2</sub> at supercritical conditions on the test gloves samples.

Test Type	Test No.	Temp. (°C)	Pressure (MPa)	CO <sub>2</sub> Density (g/mL)	Pressurisation Time (min)	Exposure Time (min)	Depressurisation Time (min)	PVAc (MW)	Co-Solvent
Safety	1	33	10	0.73834	40	30	120	-	-
	2	40	36	0.93932	10	120	5	-	-
Consolidation	3	40	28	0.89853	10	120	10	167,000	-
	4	40	28	0.89853	10	120	11	167,000	-
	5	40	28	0.89853	8	120	9	167,000	-
	6	40	28	0.89853	7	120	7	167,000	-
	7	40	36	0.93932	8	120	2	167,000	-
	8	40	36	0.93932	6	120	10	83,000	-
	9	40	36	0.93932	5	120	5	83,000	-
	10	40	36	0.93932	7	120	5.5	83,000	-
	11	40	36	0.93932	4.5	120	5.5	83,000	-
	12	40	36	0.93932	5.5	120	2	83,000	-
	13	40	36	0.93932	5	120	4.5	83,000	EtOH <sup>(1)</sup>
	14	40	36	0.93932	4.5	120	3.5	83,000	EtOH <sup>(1)</sup>
	15	40	36	0.93932	10	120	1	83,000	EtOH <sup>(1)</sup>
	16 <sup>(2)</sup>	40	36	0.93932	4	120	5.5	83,000	-
	17 <sup>(2)</sup>	40	36	0.93932	8	120	5	83,000	-
	18 <sup>(2)</sup>	40	36	0.93932	8	120	4.5	83,000	-

<sup>(1)</sup> 1 mL of ethanol (assay  $\geq$  99.8%) was added at the bottom of the high-pressure cell. <sup>(2)</sup> Three samples of approximately 10 × 15 mm were placed in the high-pressure cell and treated simultaneously.

These trials enabled a better assessment of the behaviour and response of the samples to different experimental conditions, of potential alterations primarily due to rapid pressure variations and of the suitability of the method for synthetic latex-based foams.

For the scCO<sub>2</sub>-assisted consolidation trials (Tests 3–18, Table 1), approximately 0.5 g of ground PVAc was used, a quantity that proved to be enough for the trials to be conducted in saturated conditions. Trials were performed at a fixed temperature (40 °C) and impregnation time (120 min), and variable pressure (28 MPa and 36 MPa) and depressurisation times (approximately 10, 5 and 2 min). Initial pressure values of 28 MPa were selected based on the ability to still use the sapphire windows on the high-pressure cell to monitor the samples. To achieve efficient and reproducible results, further tests were performed at higher pressure values of 36 MPa, which was the maximum pressure considered safe for the synthetic latex-based foam during safety trials, although it required the substitution of the sapphire windows for stainless-steel ones. According to the literature [21,22,26,27,69], the cloud-point pressures increase with PVAc chain length, meaning that the two PVAc compounds tested (MW 83,000 and 167,000) would possibly need higher pressure values to be completely dissolved in CO<sub>2</sub>. However, considering a polymer's molecular weight distribution (polydispersity), it is believed to be possible to solubilise and impregnate the shorter PVAc chains at the selected pressure values to successfully consolidate the foam samples.

A complete list of the experimental conditions used is summarised in Table 1.

Trials were performed in a high-pressure, laboratory-scale apparatus, as shown schematically in Figure 2.

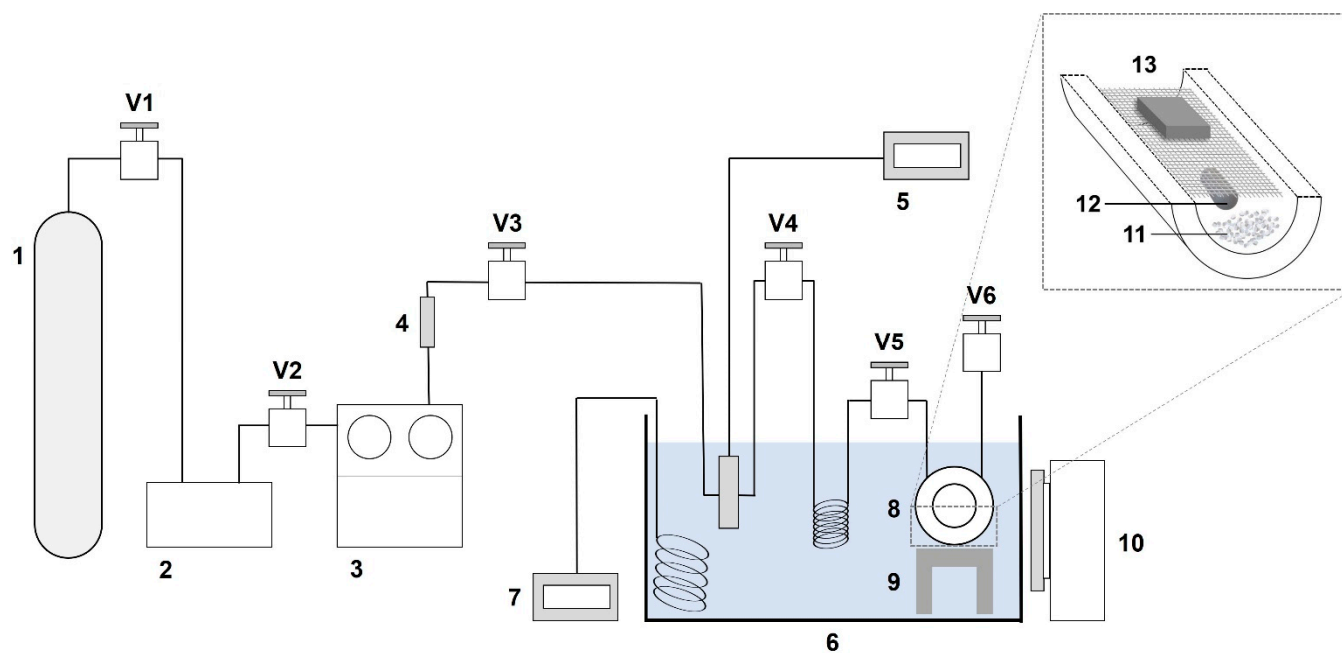


**Figure 2.** Schematic diagram showing the apparatus used for trials: (1) CO<sub>2</sub> cylinder, (2) refrigerator unit, (3) high-pressure pump, (4) check valve, (5) pressure transducer, (6) thermostatic bath, (7) temperature controller, (8) high-pressure cell, (9) cell supporter, (10) magnetic stirrer, (11) consolidant, (12) magnetic bar, (13) sample over stainless-steel grid, (V1 to V6) pressure valves.

A sample of approximately  $10 \times 15 \times 5$  mm per test (unless otherwise specified in Table 1) was placed on a stainless-steel grid support and inserted into a 33 mL stainless-steel cell. For consolidation experiments, the ground PVAc was placed at the bottom of the cell beneath the net, on the opposite side to the sample. A magnetic stirring bar was also added at the bottom of the reactor (Figure 2) to ensure the homogeneity of the CO<sub>2</sub> phase and promote the dissolution of the consolidant. The cell was sealed and immersed in a thermostatic water bath, pre-heated to the desired temperature. A BlueShadow Pump 40P (Knauer, Berlin, Germany) was used to pump fresh CO<sub>2</sub> until the desired pressure was reached inside the cell. At this point, the magnetic stirring was turned on (100 rpm), and the temperature and pressure were kept constant during the exposure time. At the end of each experiment, the cell was manually depressurised back to atmospheric pressure. Throughout experiments, different depressurisation times were tested (Table 1) to minimise consolidant removal during the exit of the CO<sub>2</sub> from the cell and to maximise the consolidant loading. Ethanol was selected as a co-solvent since it has good miscibility in scCO<sub>2</sub>, can improve the polarity of the scCO<sub>2</sub>-phase and thereby increase the solubility of polar molecules [13], as well as promote solubility of PVAc in scCO<sub>2</sub> [27,69]. In this case, 1 mL of ethanol (assay  $\geq 99.8\%$ ) was added to the bottom of the cell, and experiments were performed as discussed above. The experiments were performed in duplicate to assess the reproducibility of the method.

#### 2.4. Sample Characterisation

After trials, the treated samples were left in ambient conditions for at least 3 h prior to commencing the post-treatment assessment. The characterisation of samples was performed through a combination of empirical observation and microscopic and spectroscopic techniques, described in detail below.

##### 2.4.1. Empirical Observations

Changes in the appearance of the scCO<sub>2</sub>-exposed samples (colour, gloss and shape) were assessed visually under daylight based on observations, notes and macro photographs of the samples taken before trials and by visual comparison with untreated control samples.

Changes in the samples' dimensions were determined by imaging with the stereomicroscope, using a template mask made with millimetre-scale paper to ensure the identical positioning of the sample before and after treatment.

Qualitative evaluation of the effects of treatment on the tactile properties (such as firmness, cohesion and flexibility) was conducted by gently pinching the samples between fingers and comparing them with untreated control samples analysed in the same way.

For samples subjected to scCO<sub>2</sub>-assisted consolidation trials, the efficacy of the consolidation treatment was evaluated based on the samples' response to abrasion. This was a visual assessment achieved by rubbing a piece of Whatman filter paper number 1 (Sigma-Aldrich, St. Louis, MO, USA) across the sample surface in one direction under the light pressure of one finger [8] until noting crumbling and fragment detachment. Indirect information on the friability of the sample's surface was also provided during the micro-sampling of the model foam specimens to perform ATR-FTIR measurements. Micro-samples were taken with a sharp surgical scalpel, and it was noted that in case of unsuccessful consolidation, the surface would crumble on contact with the blade.

#### 2.4.2. Colour Measurements

For samples subjected to safety trials (Tests 1 and 2, Table 1), colourimetric measurements were also acquired to better evaluate potential colour changes induced by exposure to scCO<sub>2</sub> and the procedure's suitability for the synthetic latex-based foam.

Colourimetric measurements were performed using a Microflash mobile colourimeter (DataColor International, Lucerne, Switzerland) equipped with a Xenon lamp. The 1976 CIELAB coordinates ( $L^*$ ,  $a^*$ ,  $b^*$ ) were calculated over a 10 mm diameter measuring area, a 10° viewing angle geometry and a D65 illuminant. The instrument was calibrated with white (100% reflective) and black (0% reflective) standard plates provided by the manufacturer. Lab\* coordinates were measured in two predetermined areas per sample using a custom-made positioning mask, which enabled the collection of measurements on the same area before and after treatment. Three measurements per area were collected, and the average and standard deviation were calculated for each Lab\* coordinate, along with the variation ( $\Delta$ ) of each coordinate after treatment. Total colour variation ( $\Delta E^*$ ) was also calculated according to CIELAB 1976 ( $\Delta E^*_{ab}$ ) expression [72,73]. Colour variations are considered significantly different and can also be appreciated by the naked eye for  $\Delta E^*$  values  $\geq 2.3$  [72].

#### 2.4.3. Imaging

Samples were observed before and after treatment under an MZ16 stereomicroscope (Leica Microsystems GmbH, Wetzlar, Germany), coupled with a Leica ICD digital camera and a fibre-optic light Leica system (Leica KL 1500 LCD, Leica Microsystems GmbH, Wetzlar, Germany) and Leica FireCam software at a magnification of  $\times 10$ ,  $\times 50$  and  $\times 80$ .

Detailed images of the samples' surface were acquired using an Axioplan 2 Imaging microscope system (Zeiss, Jena, Germany), equipped with halogen (HAL 100) and mercury (N HBO 103) light sources and coupled with a DXM1200F digital camera and ACT-1 control software (Nikon Corporation, Tokyo, Japan). Microphotographs were captured within a few days from CO<sub>2</sub> exposure, using reflected (incident) light in brightfield at varied magnifications ( $\times 50$ ,  $\times 100$ ,  $\times 200$ ). Observation was also undertaken using a magnification of  $\times 500$ , which was achieved using a long working distance  $\times 50$  Olympus LMPlanFL N objective (Olympus Corporation, Tokyo, Japan).

#### 2.4.4. Attenuated Total Reflection Fourier Transform Infrared (ATR-FTIR) Spectroscopy

Infrared analysis was performed on micro-samples taken with a surgical scalpel from the synthetic latex-based foam surface, core and edge (or side), collecting at least two spectra per micro-sample.

ATR-FTIR spectra were obtained using a handheld Agilent 4300 spectrophotometer (Agilent, Santa Clara, CA, USA) equipped with a ZnSe beam splitter, a Michelson inter-



ferometer and a thermoelectrically cooled DTGS detector. Spectra were collected with a diamond ATR crystal interface, 128 scans and a resolution of  $4\text{ cm}^{-1}$  in the spectral region between  $4000$  and  $650\text{ cm}^{-1}$ . Background spectra were collected between every acquisition. The OriginPro 8 software (OriginLab Corporation, Northampton, MA, USA) was used to analyse the spectra. All spectra are presented as acquired without baseline corrections or other manipulations.

#### 2.4.5. Scanning Electron Microscopy (SEM) Imaging

Morphological analysis of the samples' surface and cross-section was performed using a Phenom ProX G6 Scanning Electron Microscope (SEM) (Thermo-Scientific, Waltham, MA, USA). Foam samples were cut with a scalpel blade into small pieces, mounted on an aluminium sample holder with double-sided carbon tape and coated with a homogeneous thin film of Au-Pd alloy using a sputtering device (Q150T ES, Quorum Technologies, East Sussex, UK). SEM observations were performed in low vacuum mode, using a large field detector (LFD) and an acceleration voltage of 15 kV.

### 3. Results and Discussion

#### 3.1. Safety Assessment: Impact of $\text{scCO}_2$ and Selected Experimental Conditions on Mock-Ups

Trials to assess a potentially negative impact of  $\text{scCO}_2$  on the foam samples were performed and revealed that exposure to  $\text{CO}_2$  at supercritical conditions neither caused alterations in the samples' appearance and tactile properties nor induced modifications at the molecular level.

For Test 1, performed at  $33\text{ }^\circ\text{C}$  and  $10\text{ MPa}$  (Table 1), it was possible to observe the specimens through the sapphire windows of the cell throughout the experiment. No visible changes, such as swelling or shrinkage, were noted in the specimen during pressurisation, exposure and depressurisation. Test 2 was performed at  $40\text{ }^\circ\text{C}$  and a much higher pressure of  $36\text{ MPa}$ , which required substituting the sapphire windows with stainless-steel ones, leading to the impossibility of monitoring the sample during the experiment. However, upon removal of the specimen from the high-pressure cell, it appeared unchanged.

For both trials, mock-ups seem to have retained their original appearance, shape and dimensions. In particular, the specimens neither shrunk under the high pressure applied, possibly due to their porous structure and existence of pore interconnectivity, nor expanded during depressurisation, suggesting that  $\text{scCO}_2$  induced no or minimal swelling of the polymers. However, it cannot be excluded that minimal variations have occurred and were not noticeable by the naked eye.

Colourimetric measurements confirmed that no alterations noticeable by the naked eye occurred, reporting average colour difference values of  $\Delta E^*_{ab}$  of 1.14 and 0.28 for Tests 1 and 2, respectively (visible colour change for  $\Delta E^*$  values  $\geq 2.3$  [72]) (Table 2).

**Table 2.** Average values and standard deviation for colour coordinates ( $L^*$ ,  $a^*$ ,  $b^*$ ) of the test samples, measured in the two predetermined areas per sample ( $\alpha$  and  $\beta$ ) before and after safety trials, and respective  $\Delta b^*$  and  $\Delta E^*_{ab}$  variations.

Test No.	Area	Before			After			Variations	
		$L^*$	$a^*$	$b^*$	$L^*$	$a^*$	$b^*$	$\Delta b^*$	$\Delta E^*_{ab}$
Test 1	$\alpha$	73.41 ( $\pm 0.10$ )	1.47 ( $\pm 0.09$ )	17.64 ( $\pm 0.21$ )	72.76 ( $\pm 0.11$ )	1.03 ( $\pm 0.04$ )	18.46 ( $\pm 0.37$ )	0.82	1.14
	$\beta$	74.72 ( $\pm 0.55$ )	1.00 ( $\pm 0.04$ )	17.94 ( $\pm 0.13$ )	74.95 ( $\pm 0.32$ )	0.86 ( $\pm 0.05$ )	19.05 ( $\pm 0.13$ )	1.10	1.14
Test 2	$\alpha$	67.88 ( $\pm 0.13$ )	13.41 ( $\pm 0.03$ )	41.94 ( $\pm 0.04$ )	67.94 ( $\pm 0.07$ )	13.40 ( $\pm 0.02$ )	42.15 ( $\pm 0.66$ )	0.21	0.22
	$\beta$	71.33 ( $\pm 0.03$ )	13.95 ( $\pm 0.03$ )	46.38 ( $\pm 0.02$ )	71.40 ( $\pm 0.07$ )	13.64 ( $\pm 0.02$ )	46.23 ( $\pm 0.02$ )	-0.14	0.35

The procedure also did not compromise the fragile surface of the specimens, and no surface disruption or material loss were noted (Figure 3), representing an enormous advantage compared to the traditional consolidation approach via brushing or facing previously tested [3]. In addition, the pre-existing network of fractures and fissures on the surface did not expand, and no new ones were created at the macroscale (Figure 3).

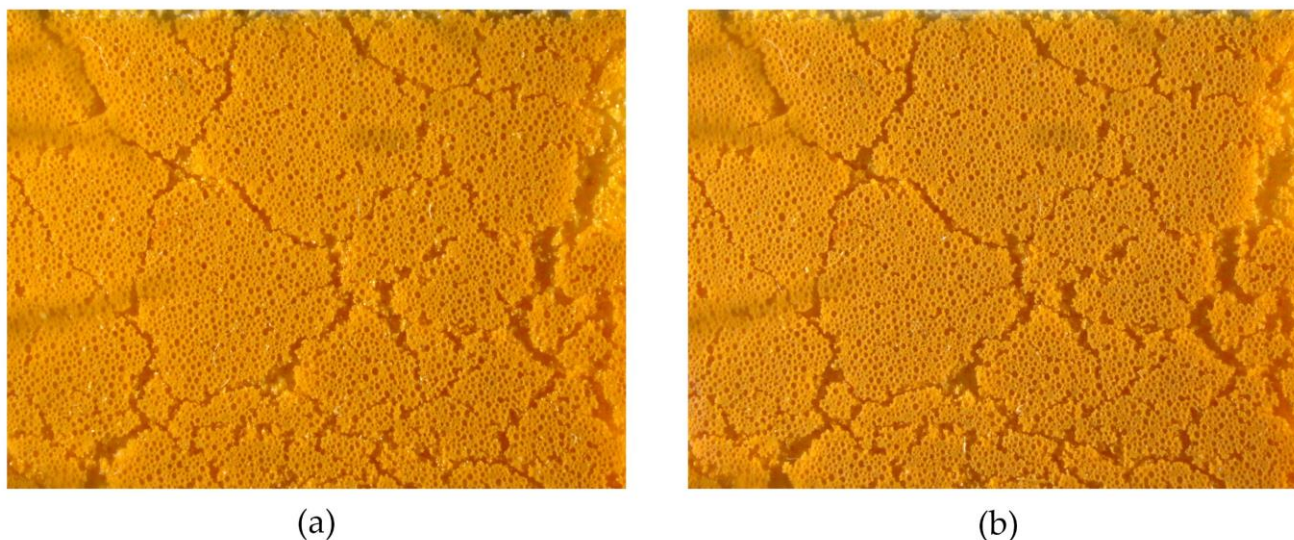


**Figure 3.** Representative photograph for a sample (a) before and (b) after exposure to supercritical CO<sub>2</sub> at 40 °C and 36 MPa (Test 2). Colour differences are due to minimal variations in the illumination setting (magnification  $\times 10$ ).

Observation at high magnification via SEM imaging also confirmed that no significant alterations occurred in the samples exposed to scCO<sub>2</sub> compared to the unexposed control (Figure 4). Both specimens exhibit smooth surfaces, and the presence of small micro-cracks (highlighted by red arrows) was detected in both unexposed and exposed samples. Although one can see a higher number of microfractures for the sample subjected to scCO<sub>2</sub> at 40 °C and 36 MPa (Test 2), these are not believed to have been caused by exposure to high pressure but are more likely due to the heterogeneous distribution of the micro-cracks throughout the foam's surface and/or due to handling and preparation of the sample before and after exposure to scCO<sub>2</sub>. Regarding the latter, it should be noted that for scCO<sub>2</sub> trials and subsequent analysis via ATR-FTIR and SEM, samples had to be cut repeatedly into smaller pieces. This proved challenging due to the intrinsic elasticity of the foam and the friability of the uppermost degraded layer.

Exposure to CO<sub>2</sub> at supercritical conditions also did not impact the tactile properties of both exposed samples, as specimens retained their original elasticity and flexibility. These properties were assessed by slightly pinching and touching the samples, with enough care to avoid inducing damage, and comparison to unexposed control samples.

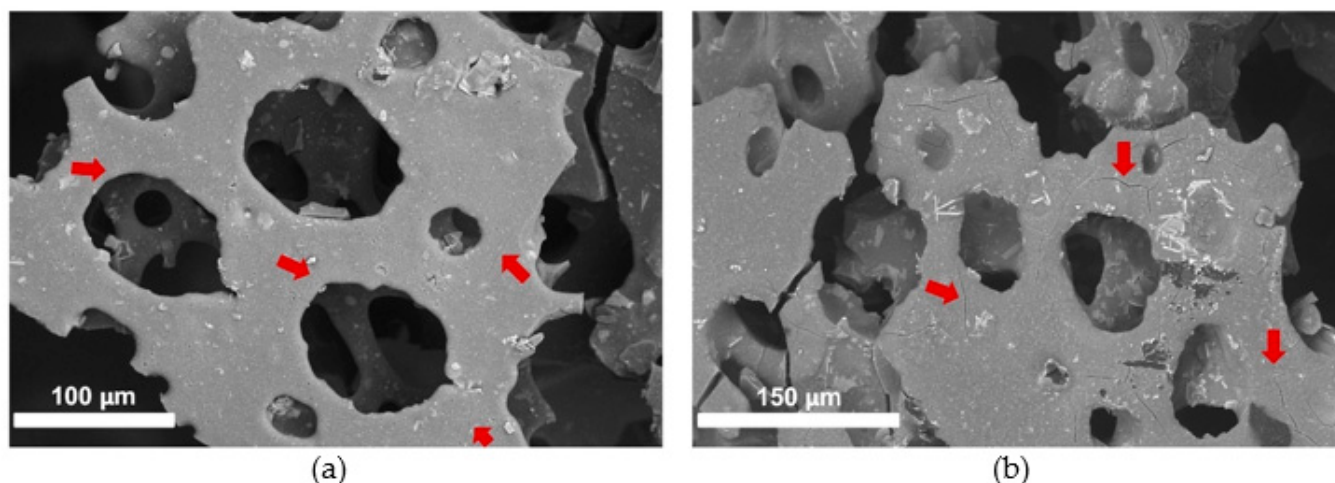


**Figure 4.** Representative SEM images for (a) control unexposed sample and (b) sample exposed to supercritical CO<sub>2</sub> at 40 °C and 36 MPa with no consolidant (Test 2). Red arrows highlight the presence of micro-cracks (magnification  $\times 1000$ ).

Finally, no alterations were detected at the molecular level via infrared spectroscopy. Figure 5 shows ATR-FTIR spectra for micro-samples taken from the top surface and core of the foam of a control unexposed specimen and the one of Test 2, exposed at 40 °C and 36 MPa (Table 1). It is noteworthy that, for these samples, the lateral surface of the foam has an identical spectral profile to the core and was treated likewise. All spectra present a similar spectral profile, which is typical of a synthetic latex-based foam composed of a mixture of poly(isoprene) and poly(butadiene-styrene) (band assignments summarised in Table 3 [74–76]). However, significant differences are noticed between the core and top surface of the foam due to a more extended degradation of the latter, with the formation of a band at approximately  $3380\text{ cm}^{-1}$ , assigned to stretching vibrations of hydroxyl functional groups, a peak at approximately  $1710\text{ cm}^{-1}$ , characteristic of ketones and aldehydes, and a shoulder at higher wavenumbers assigned to the presence of anhydrides, lactones and peracids [74,75]. Spectra acquired from the top surface and core for the samples exposed to scCO<sub>2</sub> at 40 °C and 36 MPa did not exhibit variations or shifts in absorption bands when compared to the respective area of the unexposed control specimen, suggesting that no alterations at the molecular level occurred as a result of exposure to CO<sub>2</sub> at supercritical conditions.

**Table 3.** Infrared assignment of relevant bands for polyisoprene and poly(butadiene-styrene).

Polyisoprene [74]		Poly(Butadiene-Styrene) [75]	
Wavenumber (cm <sup>-1</sup> )	Assignment	Wavenumber (cm <sup>-1</sup> )	Assignment
3036	$\nu(\text{=C-H})$	3077	$\nu(\text{C-H})$
2962	$\nu_{\text{as}}(\text{CH}_3)$	3025	$\nu(\text{C-H})$
2928	$\nu_{\text{as}}(\text{CH}_2)$	2919	$\nu_{\text{as}}(\text{CH}_3)$
2855	$\nu_{\text{s}}(\text{CH}_2)$	2845	$\nu_{\text{s}}(\text{CH}_3)$
1450	$\delta(\text{CH}_2)$	1493	$\nu(\text{aromatic ring})$
1377	$\delta_{\text{as}}(\text{CH}_3)$	1450	$\delta(\text{CH}_2)$
899	$\delta(\text{CH}_3)$	967	$\delta(\text{C-H})$ (1,4-trans)
837	$\delta(\text{=C-H})$	910	$\delta(\text{C-H})$ (1,2 vinyl)
		758	$\delta(\text{C-H})$ (phenyl groups)
		700	$\delta(\text{C-H})$ (1,4-cis)

$\nu$ —stretching;  $\delta$ —bending (scissoring); s—symmetric; as—asymmetric.

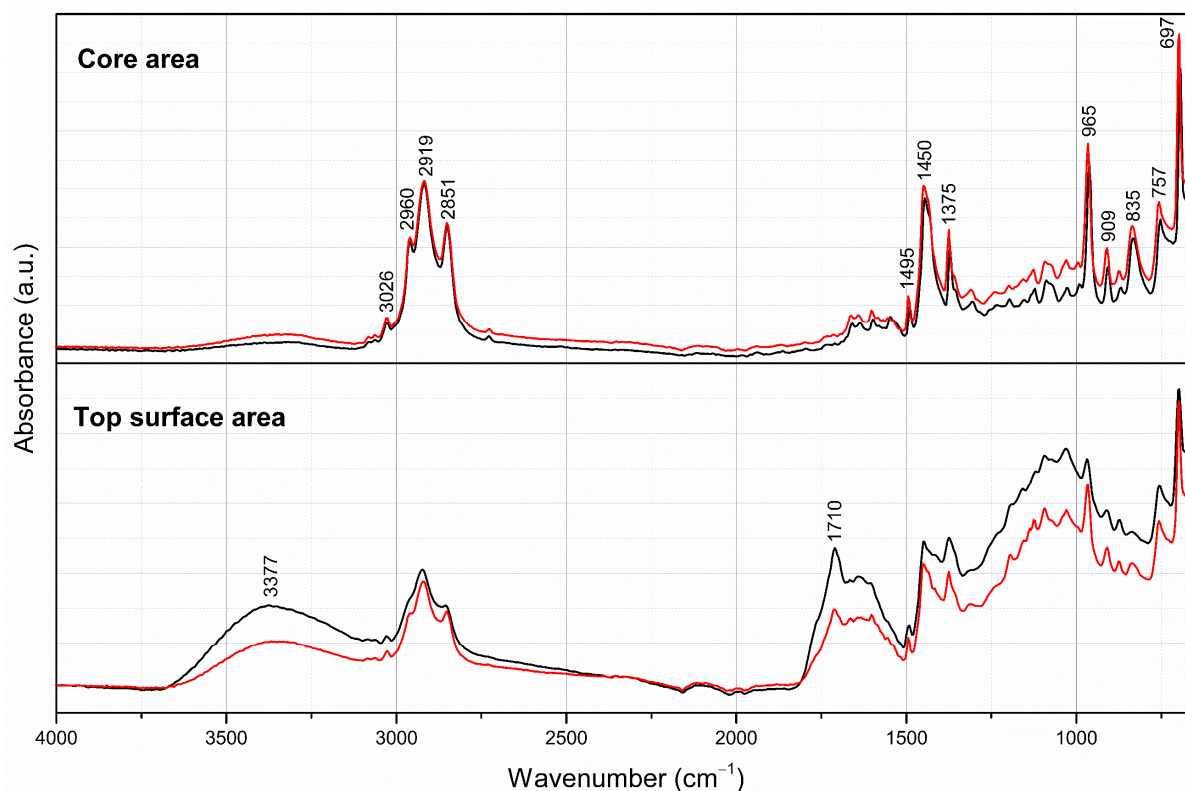


**Figure 5.** ATR-FTIR spectra of micro-samples taken from the core (**top**) and the top surface (**bottom**) of the foam of an unexposed control sample (— black line) and of a sample exposed to scCO<sub>2</sub> at 40 °C and 36 MPa (Test 2, — red line).

### 3.2. Supercritical Carbon Dioxide (CO<sub>2</sub>)-Assisted Impregnation

A summary of the samples' assessment regarding the presence of consolidant and surface cohesion after the scCO<sub>2</sub>-assisted consolidation trials is reported in Table 4.

**Table 4.** Results of analysis performed on samples subjected to scCO<sub>2</sub>-assisted consolidation trials.

Test No.	Presence of Consolidant (via ATR-FTIR)			Surface Cohesion (Empirical Obs.)
	Top Surface	Core	Lateral	
3	Y	Y	Y	Y
4	N	N	N	N
5	N	N	N	N
6	M	N	N	N
7	Y	M	N	M
8	Y	M	M	N
9	Y	M	N	Y
10	Y	M	M	Y
11	Y	M	M	Y
12	Y	M	Y	Y*
13	M	M	M	N
14	Y	M	M	Y
15	Y	Y	M	Y*
16	Y	M	Y	M
17	Y	M	M	M
18	Y	M	M	M

Y: yes; N: no; M: minimal. \* Presence of white solid deposits on the top surface, visible to the naked eye.

Initial consolidation trials (Tests 3–6, Table 1) were performed using PVAc with a MW of 167,000 at a pressure of 28 MPa, an exposure time of 120 min and similar pressurisation

and depressurisation times of approximately 10 min each. At this experimental pressure, it was possible to use the high-pressure cell with sapphire windows and thus monitor the samples throughout the experiment and observe the behaviour of the consolidant. As expected, and in agreement with the results from the safety assessment (see Section 3.1), no changes were noted in the samples' appearance, shape and dimensions after treatment. Concerning the consolidant, strong visual indicators of a possible solubilisation of the PVAc in CO<sub>2</sub> at these conditions were observed: first, a good interaction with the CO<sub>2</sub> during depressurisation leading to morphological modifications of the consolidant, more specifically, its rapid expansion and turning into a white amorphous material with a foam-like appearance due to CO<sub>2</sub> sorption (as expected for polymers [65–68]); in addition, the occurrence of the Tyndall effect during depressurisation (the inside of the cell turned from clear and colourless to cloudy orangish), strongly indicating density interferences of solubilised or dispersed material in the scCO<sub>2</sub> leading to the scattering of the light. Moreover, the presence of the consolidant in the cell after the experiments indicated they were conducted in saturated conditions, as initially intended.

The successful solubilisation of the PVAc in CO<sub>2</sub> was proven by the effective consolidation of the Test 3 sample, confirmed by analysis via optical microscopy, ATR-FTIR and friability tests (see also Table 4). However, successes were not obtained for Tests 4–6, although performed under similar conditions (same temperature and pressure values and similar pressurisation, exposure and depressurisation times).

Optical microscopy (OM) examination revealed that the Test 3–6 samples were characterised by pristine surfaces, similar to the untreated control sample (Figure 6). However, for Test 6 (Figure 6c,d), tiny rounded deposits and lumps were also noted, which might be attributed to the presence of consolidant deposited on the surface in minimal amounts. On the contrary, for Test 3 (Figure 6e,f), one can notice that the surface appears more or less homogeneously covered by a thin layer, as a “second skin”, and that some of the (smaller) pores are closed and filled with a transparent and shiny material, suggesting the presence and homogeneous deposition and distribution of the consolidant on the surface.

Friability tests highlighted an increased surface cohesion for Test 3, since no crumbling or fragment detachment was noted when rubbing the surface with the Whatman filter paper. At the same time, the sample retained its original flexibility and did not become overly rigid. On the other hand, the surfaces of the Test 4–6 samples were still very brittle, and fragments were easily removed when using the Whatman filter paper. In addition, indirect information on the cohesion of the foams was provided when taking micro-samples for ATR-FTIR analysis, which proved difficult for the Test 4–6 samples due to their fragile surface.

Infrared spectroscopy also showed significant variations in the spectral profile of Test 3 sample compared to those of Tests 4–6 and the untreated control sample, as shown in Figure 7. The top surface and core of Test 3 (Figure 7, top) sample clearly exhibit spectral signatures of PVAc (red line and highlighted by red arrows), namely the strong C=O stretching absorption band at 1730 cm<sup>-1</sup> and the fingerprint region characterised by the CH<sub>3</sub> bending at 1373 cm<sup>-1</sup>; C–O and C–C stretching at 1225 cm<sup>-1</sup>; and C–O, C–C and CH–O stretching at 1018 cm<sup>-1</sup> [71,77,78]. Whilst, for Tests 4 and 5, infrared analysis did not show any evidence of the presence of the consolidant in any of the specimens' layers, a tiny shoulder and peak were observed for Test 6 at approximately 1730 and 1240 cm<sup>-1</sup>, respectively (Figure 7, bottom), which were not present in the untreated control sample and can be attributed to PVAc. Considering that clues for its presence on the sample surface for Test 6 were also noted under OM (i.e., tiny rounded deposits and lumps on the sample's surface observed in Figure 6c,d), deposition of the consolidant possibly occurred during this experiment, but in quantities too small to provide a strengthening effect. The possibility cannot be excluded that PVAc was deposited on the surfaces of Tests 4 and 5, but in tiny amounts below the instrument detection limit that were, hence, not detected.

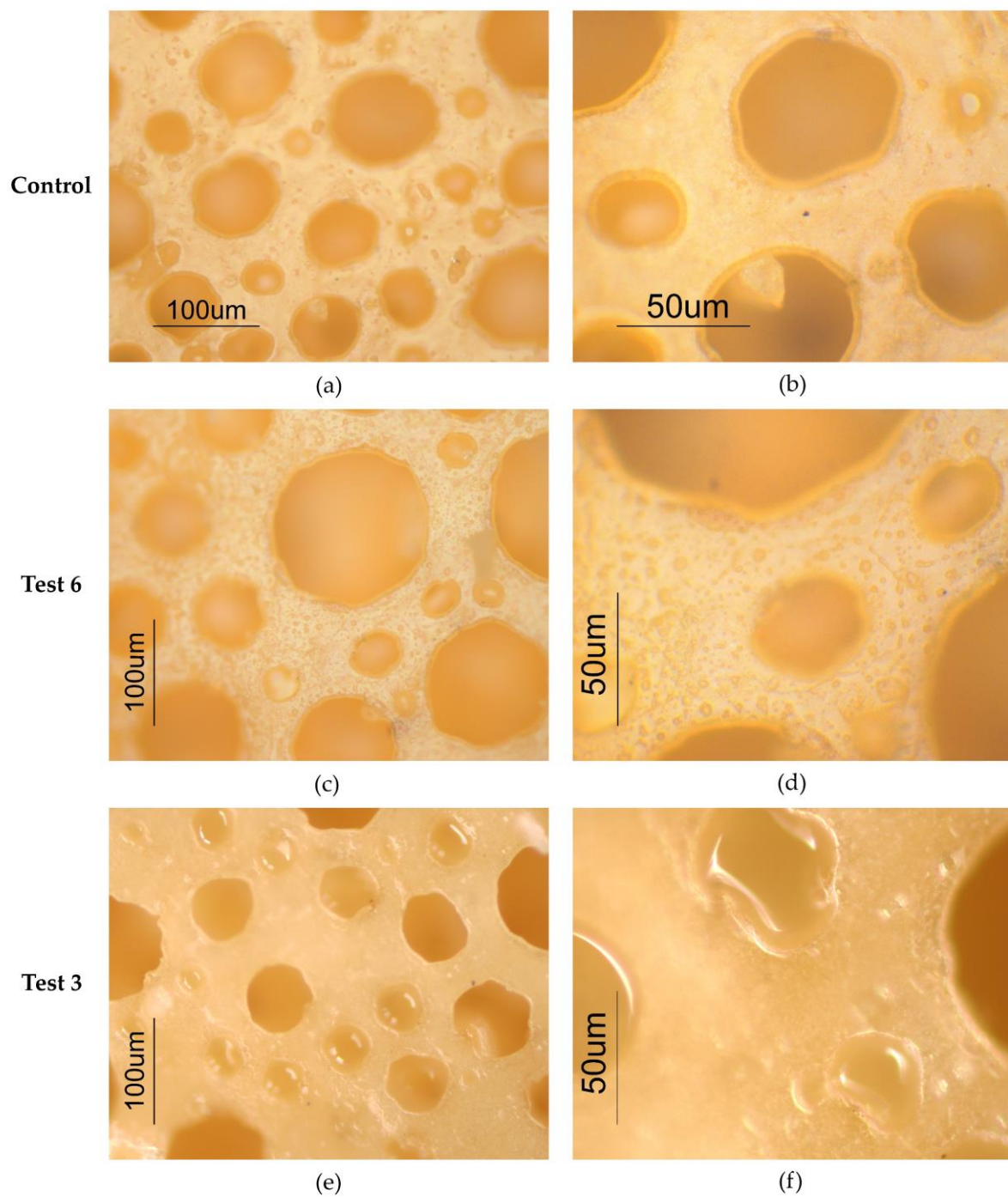


**Figure 6.** Representative microphotographs acquired in reflected light in brightfield showing the top surface for (a,b) control unexposed sample, (c,d) Test 6 and (e,f) Test 3. Magnification (left)  $\times 200$  and (right)  $\times 500$ .

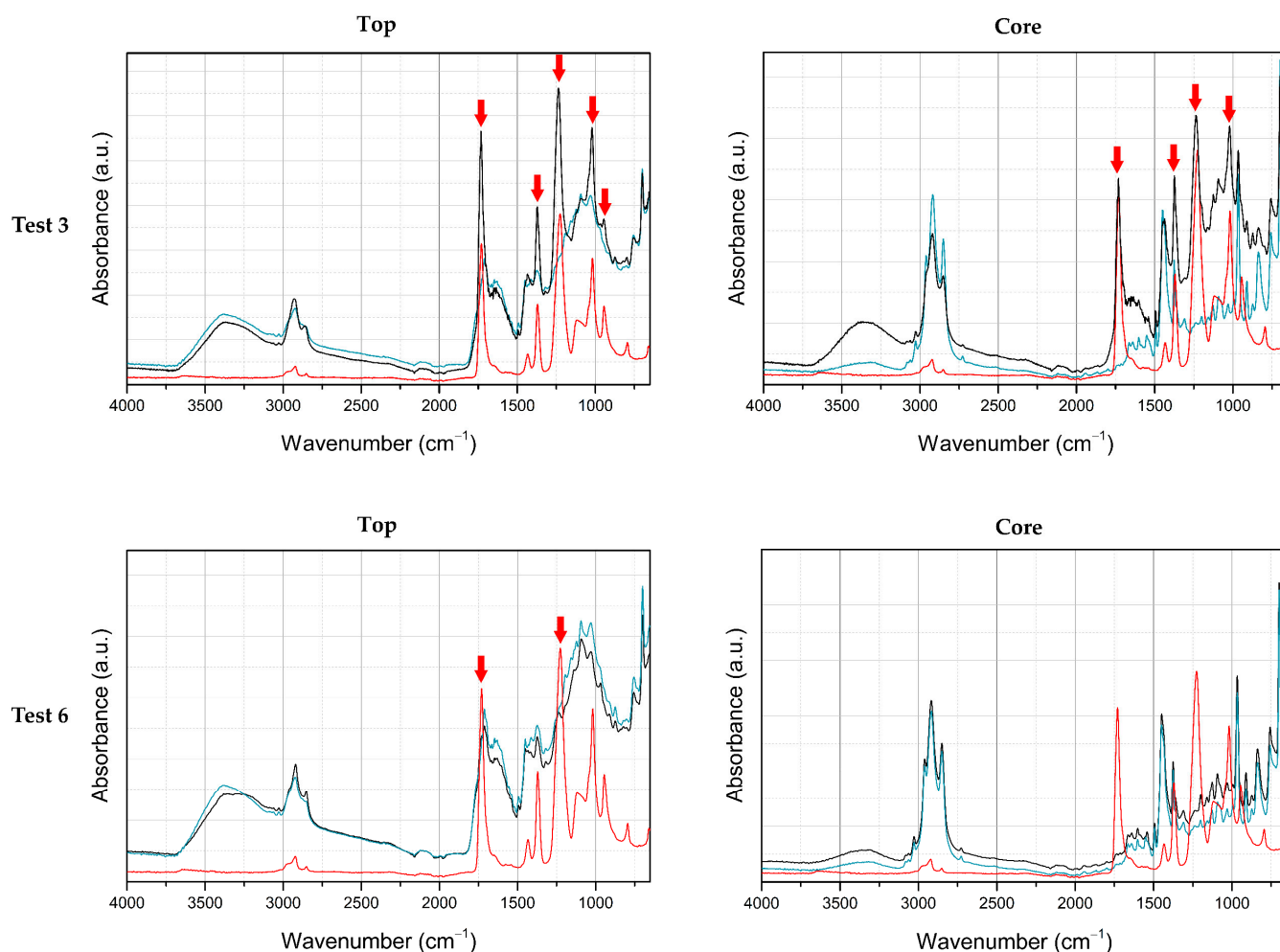


**Figure 7.** Representative ATR-FTIR spectra from micro-samples taken from the top surface and core of the foam of Tests 3 and 6 treated samples (— black line), control unexposed sample (— green line) and PVAc (— red line). Red arrows point to absorption peaks in the treated samples that may be attributed to PVAc.

Thereby, despite the similarity of the conditions used during Tests 3–6, the results show a clear difference in the extent of consolidant penetration onto the latex-based foams, highlighting a difficulty in reproducing the successful consolidation of Test 3 at these conditions. Several factors can be pointed out to possibly explain this phenomenon, such as differences in the morphology of the samples, the size of the PVAc beads and the rate of depressurisation. The morphology of the latex-based foams might influence the diffusion and deposition of the consolidant: in general, the top degraded surface is characterised by a more porous structure, whilst the less degraded areas have fewer pores of smaller size. Therefore, differences between samples might have contributed to a deeper or shallower penetration of the consolidant. In addition, the particle size of the grounded PVAc beads might have varied between experiments, which influences mass transference and ease of dissolution in  $\text{CO}_2$ . Lastly, although it was possible to control the overall time of depressurisation so that it would be the same for all tests, the speed of depressurisation was not, since it was performed manually due to a limitation of the equipment. Therefore, fluctuations in the depressurisation rate could have interfered with the amount of consolidant that remained impregnated into the foams and deposited on the surface of the samples.

Based on these results, four variables were considered and fine-tuned in order to improve the chances of success in consolidating the latex-based foams with PVAc: (i) increasing

the pressure value up to 36 MPa, (ii) using a PVAc with a lower MW (namely 83,000), (iii) assessing various depressurisation times (i.e., 10, 5 and 2 min) and (iv) the addition of ethanol as a co-solvent to improve the solubility of PVAc in CO<sub>2</sub>.

Since a successful impregnation was achieved with the higher MW PVAc, further tests were first performed by firstly increasing the experimental pressure to 36 MPa and reducing the depressurisation time to 2 min (Test 7, Table 1).

The optical microscopy examination of the Test 7 sample showed the presence of deposits of different sizes on the surface (Figure 8a), and the presence of PVAc was clearly detected on the top surface and in smaller amounts in the core of the latex-based foam by ATR-FTIR analysis (Figure 8b). However, minimal enhancement of the surface cohesion was achieved, and the sample was still crumbling.

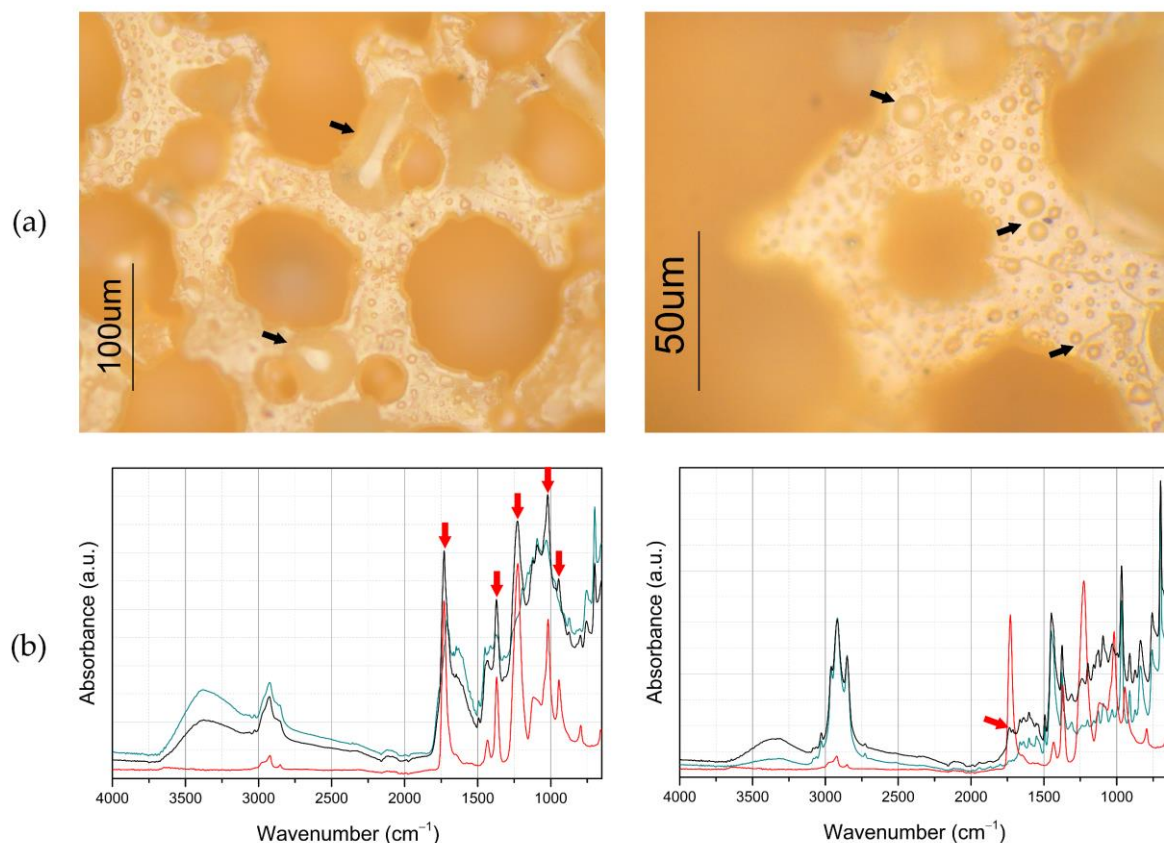


**Figure 8.** (a) Representative microphotographs acquired in reflected light in brightfield showing the top surface of the Test 7 sample. Black arrows highlight the presence of consolidant deposits on the surface. Magnification of (left)  $\times 200$  and (right)  $\times 500$ . (b) Representative ATR-FTIR spectra from micro-samples taken from (left) the top surface and (right) core of the foam of the Test 7 treated sample (— black line), control unexposed sample (— green line) and PVAc (— red line). Red arrows point to absorption peaks in the treated sample that may be attributed to PVAc.

Raising the pressure to 36 MPa and working with a PVAc with a lower molecular weight resulted in successful and reproducible results for all tests performed (Tests 8–18, Tables 1 and 4). However, differences were noted based on the depressurisation times, and shorter ones seem to increase the amount of deposited consolidant.

OM and SEM imaging show, for 10 min depressurisation (Test 8, Table 1), the presence of tiny droplets of different sizes on the sample's top surface (Figures 9a,b and 10b, respectively). For 5 min depressurisation instead (Tests 9–11, Table 1), areas with a homogeneous layer covering the sample surface and filling the smaller pores and others characterised by the presence of droplets were noted (Figures 9c,d and 10c). Finally, for 2 min depressurisation (Test 12, Table 1), a homogeneous layer covering the sample surface and filling



the smaller pores was observed (Figures 9e,f and 10d). However, at this depressurisation time, excessive expansion of the consolidant occurred, resulting in the samples' attachment to the metallic net and the presence of white solid deposits on their top surface, visible to the naked eye. The formation of deposits might be avoided using a filter to place the consolidants, as discussed by Champeau et al., 2015 [31].

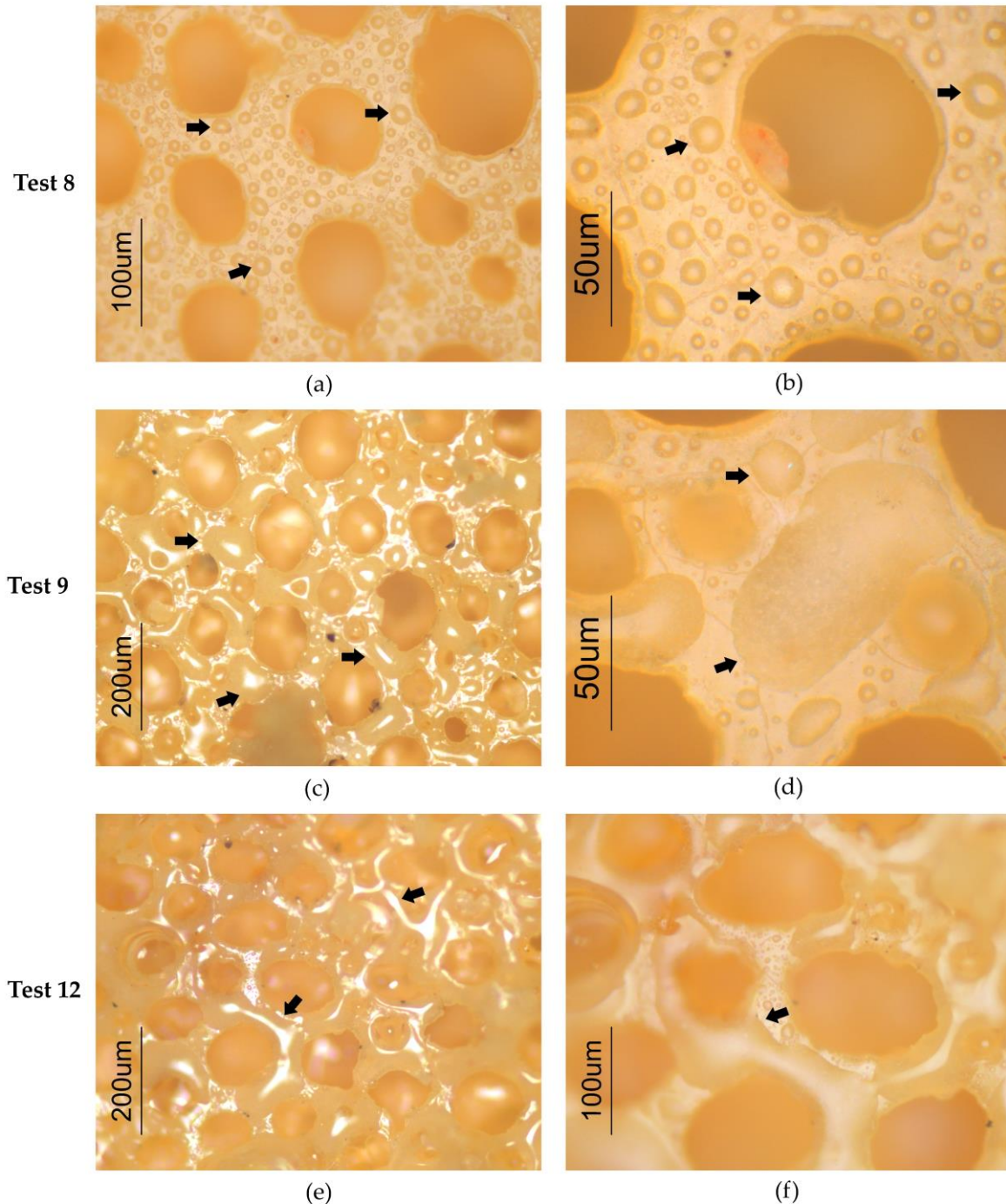


**Figure 9.** Representative microphotographs acquired in reflected light in brightfield for samples treated with consolidant at 40 °C and 36 MPa at different depressurisation times of (a,b) 10 min (Test 8), (c,d) 5 min (Test 9) and (e,f) 2 min (Test 12). Black arrows highlight the presence of consolidant deposits on the foam's surface. Magnification of (c,e)  $\times 100$ , (a,f)  $\times 200$  and (b,d)  $\times 500$ .

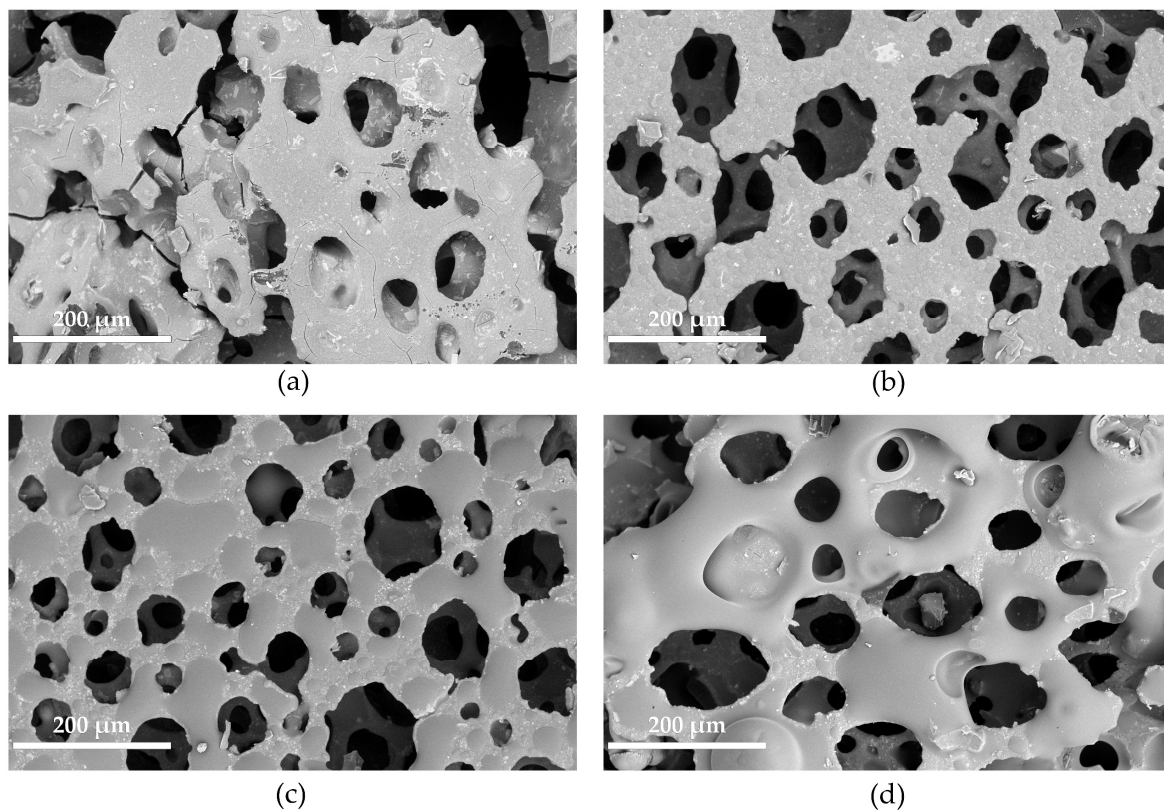


**Figure 10.** Representative SEM images showing (a) sample exposed to  $\text{scCO}_2$  at  $40\text{ }^\circ\text{C}$  and 36 MPa with no consolidant (Test 2) and samples treated with consolidant at  $40\text{ }^\circ\text{C}$  and 36 MPa with different depressurisation times of (b) 10 min (Test 8), (c) 5 min (Test 9) and (d) 2 min (Test 12). Magnification  $\times 720$ .

ATR-FTIR analysis clearly confirmed the presence of the consolidant on the top surfaces of Test 8–12 samples (treated at  $40\text{ }^\circ\text{C}$ , 36 MPa, with different depressurisation times) and in trace amounts in the core of the foams (Figure 11). In addition, infrared analysis also suggests that the amount of deposited PVAc seems to increase by reducing the depressurisation time. Moreover, concerning the cohesion of the foams, despite the detection of the presence of PVAc, the Test 8 sample (10 min depressurisation time) was not properly consolidated, as it kept crumbling when micro-samples for ATR-FTIR were taken and when the friability test was performed. On the other hand, a satisfactory enhancement of the surface cohesion was achieved for Tests 9–11 (treated at  $40\text{ }^\circ\text{C}$ , 36 MPa, with a 5 min depressurisation time). The Test 12 sample (same conditions but with a 2 min depressurisation time) seemed significantly more rigid due to deposits on its top surface, as previously stated.

At the same conditions of  $40\text{ }^\circ\text{C}$  and 36 MPa, the addition of ethanol as a co-solvent to improve the solubility of PVAc and its effect at different depressurisation times were also explored (Tests 13–15, Table 1).

By adding ethanol, the consolidant did not expand as in the previous trials during depressurisation but instead remained in a viscous state, confirming a chemical interaction with the co-solvent. For a shorter depressurisation time of 1 min (Test 15), the sample felt over-consolidated, and the deposits observed on the Test 12 sample, which was treated at similar temperature, pressure and depressurisation time but without ethanol, were not possible to avoid with the addition of the co-solvent. On the other hand, the previously successful 5 min depressurisation time without ethanol (Tests 9–11) was not enough to consolidate a sample when the co-solvent was added in the same conditions (Test 13), as the specimen was still fragile and the presence of PVAc could barely be detected by imaging and infrared analysis. A successful consolidation with ethanol was achieved when

depressurisation time was slightly reduced to fit in between the timeframe of the previous two tests (Test 14). The cohesion of the sample's surface was improved, and the presence of consolidant was confirmed by ATR-FTIR.

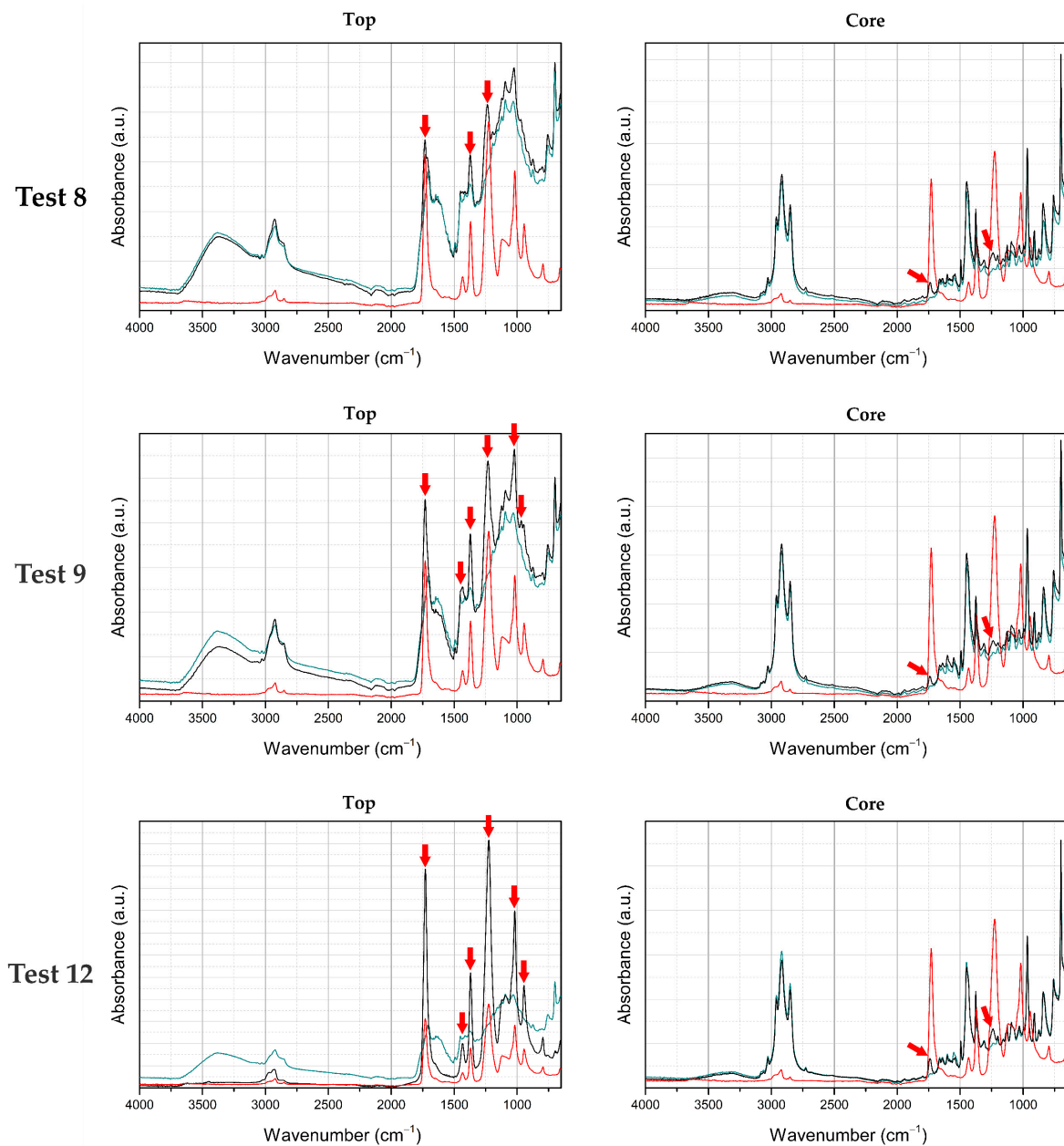


**Figure 11.** Representative ATR-FTIR spectra from micro-samples taken from the top surface and core of samples treated at 40 °C and 36 MPa, with different depressurisation times, namely: (**top row**) Test 8, 10 min; (**middle row**) Test 9, 5 min; and (**bottom row**) Test 12, 2 min. All spectra show the treated samples in black (—), control unexposed samples in green (—) and PVAc in red (—). Red arrows point to absorption peaks in the treated samples that can be attributed to PVAc.

These results indicate that the presence of ethanol might be enhancing the diffusivity of the  $scCO_2$  into the sample and, possibly, the deposition and penetration depth of the consolidant. Consequently, its presence also affects the depressurisation time required to guarantee deposition of the consolidant, as shorter times are enough to reach an adequate level of consolidation in the samples. However, ethanol might also be aiding the removal of the solubilised and deposited consolidant during depressurisation, which is

confirmed by the opposite results regarding the presence of consolidant and surface cohesion of Test 13 and Tests 9–11 (Table 4), performed at similar conditions, with and without ethanol, respectively.

Thus, the presence of ethanol did not seem to be crucial for the solubilisation of PVAc when working at these experimental conditions (40 °C and 36 MPa), as similar or better results were obtained by working without it for similar depressurisation times (for example, Tests 12 vs. 15 and Tests 9 vs. 13, Table 1). Furthermore, the only successfully consolidated sample with ethanol (Test 14) did not show a better surface cohesion than the previous successful tests performed without its addition.

The preliminary results of this study suggest that, besides the impregnation of the PVAc into the samples during the exposure time, consolidation might have also occurred via precipitation of the consolidant on the latex-based foams during depressurisation. This suggestion is based on the observation of white deposits on the top surface of some samples, namely Tests 12 and 15. Moreover, the results of ATR-FTIR analysis (Table 4) also show that, for most samples where the consolidant was detected on the top surface, it was barely present on the laterals. This precipitation phenomenon occurs due to a decrease in solubility of the PVAc in CO<sub>2</sub> when the pressure is brought back from supercritical conditions to atmospheric values during depressurisation.

Considering that experimental conditions enabling optimum and reproducible results were found (Tests 9–11, treated at 40 °C, 36 MPa and 5 min depressurisation time), further tests focused on repeating the successful trial by treating three samples simultaneously instead of one at similar conditions (Tests 16–18). In this case, however, only a minimum increase in the surface cohesion was obtained in all tests, potentially due to the limited solubility of PVAc and the fact that the solubilised fraction was equally distributed over three samples rather than one. Further trials with increased exposure time might produce similar results to the successful ones obtained in Tests 9–11. These tests highlight the need for further research into scaling up the process to larger samples in order to find an appropriate consolidation treatment for real case objects. In addition, it is important to emphasise that, although this study was conducted in a laboratory-scale apparatus with a 33 mL stainless-steel cell, larger samples and/or real case objects may be treated in available high-pressure vessels with appropriate size.

#### 4. Conclusions

This study tested the scCO<sub>2</sub>-assisted impregnation process for the first time as an alternative approach to traditional methods for consolidating synthetic latex-based foam objects. Namely, the procedure was assessed for a pair of goalkeeper gloves in the collection of Museu Benfica–Cosme Damião (Lisbon, Portugal), made of a blend of polyisoprene, polybutadiene and polystyrene, with the last two possibly as a copolymer. The presented study aimed to overcome the drawbacks and limitations of previously performed consolidation trials via facing and nebulisation [3], by eliminating the need for direct contact with the material for the deposition of the consolidant, which can lead to material losses, while still potentially achieving an in-depth and homogeneous consolidation.

Trials were performed on mock-up samples prepared using modern equivalent materials, and poly(vinyl acetate) (PVAc) was selected as a suitable consolidant due to its already-known solubility and behaviour in scCO<sub>2</sub>. Several experimental variables were considered, such as pressure, the consolidant's molecular weight, depressurisation time, and addition of ethanol as a co-solvent.

The exposure to high pressure (up to 36 MPa) and the scCO<sub>2</sub> consolidation procedure proved compatible with the synthetic latex-based foam. Alongside no alterations in the visual aesthetic, no changes to the dimensions or shape of the samples were observed due to high pressure and rapid pressure variations (i.e., swelling or shrinkage). The spectral profile also remained unchanged, suggesting that no alterations at the molecular level occurred. In addition, no disruption or material loss from the friable surface were noted, representing an enormous advantage of the scCO<sub>2</sub>-assisted consolidation compared to the

traditional techniques via facing/brushing, in which direct contact with the material is needed for the application of the consolidant.

Consolidation trials also showed that scCO<sub>2</sub>-assisted consolidation technology could be a viable alternative to traditional methods to perform consolidation treatments on foam objects of historical value, as with the appropriate experimental conditions it was possible to achieve a safe homogeneous deposition of the consolidant, i.e., with no material loss.

For trials conducted at 40 °C and 28 MPa, with a 10 min depressurisation time and PVAc with MW of 167,000, it was not possible to achieve reproducible results. A satisfactory consolidation was achieved for one test only (Test 3) out of four. This sample retained its original appearance and flexibility, whilst an increased cohesion of the surface was registered via friability tests. The presence of PVAc on the surface and in the core of the sample was clearly detected via OM and ATR-FTIR analysis. However, the deposition of the consolidant in other samples treated at the same temperature and pressure and similar pressurisation, exposure and depressurisation times (Tests 4–6) occurred in minor amounts and did not successfully strengthen the sample. Increasing the experimental pressure to 36 MPa and reducing the depressurisation time to 2 min led to the same unsatisfactory results.

On the contrary, increasing the pressure up to 36 MPa and working with a PVAc with a MW of 83,000 enabled reproducible results. Several depressurisation times were tested, and optimum results were achieved with 5 min time (Tests 9–11). In these conditions, a homogeneous deposition of the consolidant on the surface was achieved, as well as penetration into the foam, and samples showed increased mechanical strength and surface cohesion, retaining the mock-up appearance unchanged. Shorter depressurisation times of 2 min (Test 12) led to the presence of white solid deposits on the surface of the samples (also visible by the naked eye). In contrast, in longer times (10 min, Test 8), the quantity of consolidant deposited on the surface was insufficient to properly consolidate and improve the surface cohesion of the foam, leaving it still crumbling and fragile.

Alongside promising results, further research is still needed to scale up with satisfactory results the scCO<sub>2</sub>-assisted consolidation process to larger samples, to enable the possibility of treating real-scale items. Future work should involve the validation of the method in naturally aged samples with no historical value that replicate more accurately the condition of the original pair of goalkeeper gloves and also in mock-up samples that mimic the composite and complex nature of the item as a whole. Additionally, future research should address the long-term stability and efficacy of the treatment on the consolidated foam samples. Research is also ongoing involving the study of the solubility of different consolidants, including those used for PUR foams, such as alkoxy-silanes.

As the present study proved the safety and suitability of the scCO<sub>2</sub>-assisted consolidation for synthetic latex-based foams, it might represent a turning point in the conservation of foam-based historical objects as a non-toxic and potentially more efficient alternative to traditional methods, with no material losses. Experiments are also being performed to test the feasibility of this procedure for those based on polyurethane. The validation of these preliminary outcomes can pave the way for new conservation treatment options for foam-based objects, which are some of the most problematic and less studied materials in the heritage conservation field.

**Author Contributions:** Conceptualization, J.L.F. and T.C.; methodology, A.B., J.T.F., S.F.d.S., T.C. and J.L.F.; validation, A.B., J.T.F., S.F.d.S., Y.S., A.Q., T.C. and J.L.F.; formal analysis, A.B. and J.T.F.; investigation, A.B. and J.T.F.; resources, J.L.F. and T.C.; data curation, A.B. and J.T.F.; writing—original draft preparation, A.B. and J.T.F.; writing—review and editing, A.B., J.T.F., S.F.d.S., Y.S., A.Q., T.C. and J.L.F.; visualization, A.B. and J.T.F.; supervision, T.C. and J.L.F.; project administration, J.L.F.; funding acquisition, J.L.F. and T.C. All authors have read and agreed to the published version of the manuscript.

**Funding:** This research was financed by Fundação para a Ciência e a Tecnologia, Ministério da Ciência, Tecnologia, e Ensino Superior (FCT/MCTES), Portugal, through the funded research project “PlasCO<sub>2</sub>–Green CO<sub>2</sub> Technologies for the Cleaning of Plastics in Museums and Heritage Collections”

(PTDC/ARTOUT/29692/2017) and the Associate Laboratory for Green Chemistry (LAQV) financed by national funds (UIDB/50006/2020 and UIDP/50006/2020).

**Institutional Review Board Statement:** Not applicable.

**Informed Consent Statement:** Not applicable.

**Data Availability Statement:** The original contributions presented in the study are included in the article, further inquiries can be directed to the corresponding authors.

**Acknowledgments:** The authors would like to thank all the PlasCO<sub>2</sub> project team members, in particular to Ana Isabel Aguiar-Ricardo, Ana Maria Ramos (Department of Chemistry, LAQV-REQUIMTE, FCT NOVA) and Filipe Teixeira (CQUM, Universidade do Minho), and also to Thea van Oosten (independent senior conservation scientist/adviser, Amsterdam, The Netherlands), for the fruitful discussion; Isabel Pombo Cardoso (Department of Conservation and Restoration, LAQV-REQUIMTE, FCT NOVA) and Isabel Nogueira (MicroLab, IST-UL) for the assistance with optical microscopy and SEM imaging, respectively.

**Conflicts of Interest:** The authors declare no conflicts of interest. The funders had no role in the design of the study; in the collection, analyses, or interpretation of data; in the writing of the manuscript; or in the decision to publish the results.

## References

- Flexer, G.; Spring, K. Approaching the Preservation of Polyurethane Soles on Football Boots. In *Plastics in Peril: Focus on Conservation of Polymeric Materials in Cultural Heritage, Virtual Conference*. Available online: [https://www.youtube.com/watch?v=Nz\\_zbg\\_Zq4o&list=PLDhExi\\_byiwnJwb4Nx3Z3Xk5SefFvBCdx&index=9&pp=iAQB](https://www.youtube.com/watch?v=Nz_zbg_Zq4o&list=PLDhExi_byiwnJwb4Nx3Z3Xk5SefFvBCdx&index=9&pp=iAQB) (accessed on 6 February 2024).
- Ferreira, J.T. Supercritical CO<sub>2</sub> Based Green Technologies for the Consolidation of Foams in Cultural Heritage. The Case Study of Robert Enke's Pair of Gloves. Master's Thesis, NOVA School of Science and Technology, Universidade NOVA de Lisboa, Almada, Portugal, 2020. Available online: <http://hdl.handle.net/10362/113703> (accessed on 6 February 2024).
- Bartoletti, A.; França de Sá, S.; Ferreira, J.T.; Ferreira, J.L. Exploring Conservation Options for a Pair of Foam-Based Goalkeeper Gloves Belonging to Museu Benfica—Cosme Damião. In *Future Talks 021—Smart Solutions in the Conservation of the Modern*; Bechthold, T., Ed.; Die Neue Sammlung—The Design Museum: Munich, Germany, 2023; pp. 60–69.
- van Oosten, T. *PUR Facts: Conservation of Polyurethane Foam in Art and Design*; Amsterdam University Press—RCE Publications: Amsterdam, The Netherlands, 2011; ISBN 978-90-485-1207-2.
- Pellizzi, E.; Lattuati-Derieux, A.; de Lacaillerie, J.-B.E.; Lavédrine, B.; Cheradame, H. Reinforcement Properties of 3-Aminopropylmethyl-diethoxysilane and N-(2-Aminoethyl)-3-Aminopropylmethyl-dimethoxysilane on Polyurethane Ester Foam. *Polym. Degrad. Stab.* **2012**, *97*, 2340–2346. [[CrossRef](#)]
- Pellizzi, E.; Lattuati-Derieux, A.; de Lacaillerie, J.-B.E.; Lavédrine, B.; Cheradame, H. Consolidation of Artificially Degraded Polyurethane Ester Foam with Aminoalkylalkoxysilanes. *Polym. Degrad. Stab.* **2016**, *129*, 106–113. [[CrossRef](#)]
- Daher, C.; Fabre-Francke, I.; Balcar, N.; Barabant, G.; Cantin, S.; Fichet, O.; Chéradame, H.; Lavédrine, B.; Lattuati Derieux, A. Consolidation of Degraded Polyurethane Foams by Means of Polysiloxane Mixtures: Polycondensation Study and Application Treatment. *Polym. Degrad. Stab.* **2018**, *158*, 92–101. [[CrossRef](#)]
- van Aubel, C.; de Groot, S.; van Keulen, H.; Sniijders, E. Digging into the Past of Nature Carpets: The Evaluation of Treatments on Artworks by Piero Gilardi Made from Polyurethane Ether Foam. *J. Cult. Herit.* **2019**, *35*, 271–278. [[CrossRef](#)]
- Chaumat, G.; Tran, K.; Dekkers, J.M.; Pellizzi, E.; Lattuati-Derieux, A. On-Going Studies in Consolidation of Polyurethane (PUR) Foams. In *Preservation of Plastic Artefacts in Museum Collections (POPART)*; Lavédrine, B., Fournier, A., Martin, G., Eds.; Comité des Travaux Historiques et Scientifiques (CTHS): Paris, France, 2012; pp. 271–293.
- Köppen, J.; Brunner, S.; Gómez-Sánchez, E. Shoemaker's Nightmare: Deterioration of Shoe Soles and Tests for the Conservation of Degraded Closed-Cell Polyester Urethane Museum Objects. In *Future Talks 019—Surfaces. Lectures and Workshops on the Conservation of the Modern*; Bechthold, T., Ed.; Die Neue Sammlung—The Design Museum: Munich, Germany, 2021; pp. 95–102.
- Weidner, E. Impregnation via Supercritical CO<sub>2</sub>—What We Know and What We Need to Know. *J. Supercrit. Fluids* **2018**, *134*, 220–227. [[CrossRef](#)]
- Brunner, G. *Gas Extraction—An Introduction to Fundamentals of Supercritical Fluids and the Application to Separation Processes*; Baumgärtel, H., Franck, E.U., Grünbein, W., Eds.; Topics in Physical Chemistry; Steinkopff Heidelberg: Heidelberg, Germany, 1994; Volume 4, ISBN 978-3-662-07382-7.
- Clifford, T. *Fundamentals of Supercritical Fluids*; Oxford University Press: Oxford, UK, 1998; ISBN 978-0-19-850137-4.
- Belinsky, M.R. (Ed.) *Supercritical Fluids*; Nova Science Publishers, Incorporated: New York, NY, USA, 2010; ISBN 978-1-60741-930-3.
- Zhang, X.; Heinonen, S.; Levänen, E. Applications of Supercritical Carbon Dioxide in Materials Processing and Synthesis. *RSC Adv.* **2014**, *4*, 61137–61152. [[CrossRef](#)]
- Weingärtner, H.; Franck, E.U. Supercritical Water as a Solvent. *Angew. Chem. Int. Ed.* **2005**, *44*, 2672–2692. [[CrossRef](#)] [[PubMed](#)]

17. Kemmere, M.F.; Meyer, T. (Eds.) *Supercritical Carbon Dioxide: In Polymer Reaction Engineering*; Wiley-VCH Verlag GmbH & Co. KGaA: Weinheim, Germany, 2005; ISBN 978-3-527-31092-0.
18. Capello, C.; Fischer, U.; Hungerbühler, K. What Is a Green Solvent? A Comprehensive Framework for the Environmental Assessment of Solvents. *Green Chem.* **2007**, *9*, 927–934. [[CrossRef](#)]
19. Hayden, E.P. (Ed.) *Supercritical Carbon Dioxide. In Functions and Applications*; Nova Science Publishers, Incorporated: New York, NY, USA, 2020; ISBN 978-1-5361-7404-5.
20. Hrnčič, M.K.; Cör, D.; Verboten, M.T.; Knez, Ž. Application of Supercritical and Subcritical Fluids in Food Processing. *Food Qual. Saf.* **2018**, *2*, 59–67. [[CrossRef](#)]
21. Rindfleisch, F.; DiNoia, T.P.; McHugh, M.A. Solubility of Polymers and Copolymers in Supercritical CO<sub>2</sub>. *J. Phys. Chem.* **1996**, *100*, 15581–15587. [[CrossRef](#)]
22. Kirby, C.F.; McHugh, M.A. Phase Behavior of Polymers in Supercritical Fluid Solvents. *Chem. Rev.* **1999**, *99*, 565–602. [[CrossRef](#)]
23. McHugh, M.A. Solubility of Polymers in Supercritical Carbon Dioxide. In *Green Chemistry Using Liquid and Supercritical Carbon Dioxide*; DeSimone, J., Tumas, W., Eds.; Oxford University Press: New York, NY, USA, 2003; pp. 125–133; ISBN 978-0-19-515483-2.
24. Sadowski, G. Phase Behavior of Polymer Systems in High-Pressure Carbon Dioxide. In *Supercritical Carbon Dioxide: In Polymer Reaction Engineering*; Kemmere, M.F., Thierry, M., Eds.; WILEY-VCH Verlag GmbH & Co. KGaA: Weinheim, Germany, 2005; pp. 15–35.
25. Škerget, M.; Knez, Ž.; Knez-Hrnčič, M. Solubility of Solids in Sub- and Supercritical Fluids: A Review. *J. Chem. Eng. Data* **2011**, *56*, 694–719. [[CrossRef](#)]
26. Shen, Z.; McHugh, M.A.; Xu, J.; Belardi, J.; Kilic, S.; Mesiano, A.; Bane, S.; Karnikas, C.; Beckman, E.; Enick, R. CO<sub>2</sub>-Solubility of Oligomers and Polymers That Contain the Carbonyl Group. *Polymer* **2023**, *44*, 1491–1498. [[CrossRef](#)]
27. Zhu, T.; Gong, H.; Dong, M.; Yang, Z.; Guo, C.; Liu, M. Phase Equilibrium of PVAc + CO<sub>2</sub> Binary Systems and PVAc + CO<sub>2</sub> + Ethanol Ternary Systems. *Fluid Phase Equilib.* **2018**, *458*, 264–271. [[CrossRef](#)]
28. Bach, E.; Cleve, E.; Schollmeyer, E. Past, Present and Future of Supercritical Fluid Dyeing Technology—An Overview. *Rev. Prog. Color. Relat. Top.* **2002**, *32*, 88–102. [[CrossRef](#)]
29. Banchero, M. Supercritical Fluid Dyeing of Synthetic and Natural Textiles—A Review. *Color. Technol.* **2013**, *129*, 2–17. [[CrossRef](#)]
30. Duarte, A.R.C.; Simplicio, A.L.; Vega-González, A.; Subra-Paternault, P.; Coimbra, P.; Gil, M.H.; de Sousa, H.C.; Duarte, C.M.M. Supercritical Fluid Impregnation of a Biocompatible Polymer for Ophthalmic Drug Delivery. *J. Supercrit. Fluids* **2007**, *42*, 373–377. [[CrossRef](#)]
31. Champeau, M.; Thomassin, J.-M.; Tassaing, T.; Jérôme, C. Drug Loading of Polymer Implants by Supercritical CO<sub>2</sub> Assisted Impregnation: A Review. *J. Control. Release* **2015**, *209*, 248–259. [[CrossRef](#)]
32. Trindade Coutinho, I.; Champeau, M. Synergistic Effects in the Simultaneous Supercritical CO<sub>2</sub> Impregnation of Two Compounds into Poly(L- Lactic Acid) and Polyethylene. *J. Supercrit. Fluids* **2020**, *166*, 105019. [[CrossRef](#)]
33. Gurina, D.L.; Budkov, Y.A.; Kiselev, M.G. Impregnation of Poly(Methyl Methacrylate) with Carbamazepine in Supercritical Carbon Dioxide: Molecular Dynamics Simulation. *J. Phys. Chem. B* **2020**, *124*, 8410–8417. [[CrossRef](#)]
34. Meneses, L.; Craveiro, R.; Jesus, A.R.; Reis, M.A.M.; Freitas, F.; Paiva, A. Supercritical CO<sub>2</sub> Assisted Impregnation of Ibuprofen on Medium-Chain-Length Polyhydroxyalkanoates (Mcl-PHA). *Molecules* **2021**, *26*, 4772. [[CrossRef](#)] [[PubMed](#)]
35. Zhu, W.; Long, J.; Shi, M. Resveratrol-Loaded Diacetate Fiber by Supercritical CO<sub>2</sub> Fluid Assisted Impregnation. *Materials* **2022**, *15*, 5552. [[CrossRef](#)]
36. Machado, N.D.; Mosquera, J.E.; Martini, R.E.; Goñi, M.L.; Gañán, N.A. Supercritical CO<sub>2</sub>-Assisted Impregnation/Deposition of Polymeric Materials with Pharmaceutical, Nutraceutical, and Biomedical Applications: A Review (2015–2021). *J. Supercrit. Fluids* **2022**, *191*, 105763. [[CrossRef](#)]
37. Machado, N.D.; Mosquera, J.E.; Martini, R.E.; Goñi, M.L.; Gañán, N.A. Supercritical CO<sub>2</sub>-Assisted Impregnation of Cellulose Microparticles with R-Carvone: Effect of Process Variables on Impregnation Yield. *J. Supercrit. Fluids* **2022**, *188*, 105671. [[CrossRef](#)]
38. Acda, M.N.; Morrell, J.J.; Levien, K.L. Supercritical Fluid Impregnation of Selected Wood Species with Tebuconazole. *Wood Sci. Technol.* **2001**, *35*, 127–136. [[CrossRef](#)]
39. Muin, M.; Adachi, A.; Inoue, M.; Yoshimura, T.; Tsunoda, K. Feasibility of Supercritical Carbon Dioxide as a Carrier Solvent for Preservative Treatment of Wood-Based Composites. *J. Wood Sci.* **2003**, *49*, 65–72. [[CrossRef](#)]
40. Kang, S.-M.; Levien, K.L.; Morrell, J.J. Supercritical Fluid Impregnation of Wood with Biocides Using Temperature Reduction to Induce Deposition. *Wood Sci. Technol.* **2005**, *39*, 328–338. [[CrossRef](#)]
41. Aroso, I.M.; Duarte, A.R.C.; Pires, R.R.; Mano, J.F.; Reis, R.L. Cork Processing with Supercritical Carbon Dioxide: Impregnation and Sorption Studies. *J. Supercrit. Fluids* **2015**, *104*, 251–258. [[CrossRef](#)]
42. Zhang, J.; Yang, L.; Liu, H. Green and Efficient Processing of Wood with Supercritical CO<sub>2</sub>: A Review. *Appl. Sci.* **2021**, *11*, 3929. [[CrossRef](#)]
43. Yang, L.; Xu, W.Z.; Zomaya, D.; Charpentier, P.A. Softwood Impregnation by MMA Monomer Using Supercritical CO<sub>2</sub>. *J. Supercrit. Fluids* **2022**, *189*, 105712. [[CrossRef](#)]
44. Singh, M.; Dey, E.S.; Bhand, S.; Dicko, C. Supercritical Carbon Dioxide Impregnation of Gold Nanoparticles Demonstrates a New Route for the Fabrication of Hybrid Silk Materials. *Insects* **2021**, *13*, 18. [[CrossRef](#)]

45. Rojas, A.; Torres, A.; José Galotto, M.; Guarda, A.; Julio, R. Supercritical Impregnation for Food Applications: A Review of the Effect of the Operational Variables on the Active Compound Loading. *Crit. Rev. Food Sci. Nutr.* **2020**, *60*, 1290–1301. [[CrossRef](#)] [[PubMed](#)]
46. Lucic Skoric, M.; Milovanovic, S.; Zizovic, I.; Ortega-Toro, R.; Santagata, G.; Malinconico, M.; Kalagasidis Krusic, M. Supercritical CO<sub>2</sub> Impregnation of Thymol in Thermoplastic Starch-Based Blends: Chemico-Physical Properties and Release Kinetics. *Polymers* **2022**, *14*, 4360. [[CrossRef](#)] [[PubMed](#)]
47. Von Ulmann, A. Non-Polluting Removal of Pesticides from Historic Textiles—A Project at the Germanisches Nationalmuseum Nürnberg and the Deutsh Bundesstiftung Umwelt (1999–2001). In Proceedings of the Cultural Heritage Research: A Pan-European Challenge, Proceedings of the 5th EC Conference, Cracow, Poland, 16–18 May 2002; Kozłowski, R., Ed.; Institute of Catalysis and Surface Chemistry, Polish Academy of Sciences: Cracow, Poland, 2002; pp. 334–336.
48. Sousa, M.; Melo, M.J.; Casimiro, T.; Aguiar-Ricardo, A. The Art of CO<sub>2</sub> for Art Conservation: A Green Approach to Antique Textile Cleaning. *Green Chem.* **2007**, *9*, 943. [[CrossRef](#)]
49. Frade, C.S.C.; Cruz, P.; Lopes, E.; Sousa, M.M.; Hallett, J.; Santos, R.; Aguiar-Ricardo, A.; Casimiro, T. Cleaning Classical Persian Carpets with Silk and Precious Metal Thread: Conservation and Ethical Considerations. In Proceedings of the ICOM Committee for Conservation 16th Triennial Meeting, Lisbon, Portugal, 19–23 September 2011; Critério Artes Gráficas, Lda; ICOM Committee for Conservation: Almada, Portugal, 2011.
50. Aslanidou, D.; Tsiptsias, C.; Panayiotou, C. A Novel Approach for Textile Cleaning Based on Supercritical CO<sub>2</sub> and Pickering Emulsions. *J. Supercrit. Fluids* **2013**, *76*, 83–93. [[CrossRef](#)]
51. Aslanidou, D.; Karapanagiotis, I.; Panayiotou, C. Tuneable Textile Cleaning and Disinfection Process Based on Supercritical CO<sub>2</sub> and Pickering Emulsions. *J. Supercrit. Fluids* **2016**, *118*, 128–139. [[CrossRef](#)]
52. Selli, E.; Langè, E.; Mossa, A.; Testa, G.; Seves, A. Preservation Treatments of Aged Papers by Supercritical Carbon Dioxide. *Macromol. Mater. Eng.* **2000**, *280–281*, 71–75. [[CrossRef](#)]
53. Dobrodszkaya, T.V.; Egoyants, P.A.; Ikonnikov, V.K.; Romashenkova, N.D.; Sirotn, S.A.; Dobrusina, S.A.; Podgornaya, N.I. Treatment of Paper with Basic Agents in Alcohols and Supercritical Carbon Dioxide to Neutralize Acid and Prolong Storage Time. *Russ. J. Appl. Chem.* **2004**, *77*, 2017–2021. [[CrossRef](#)]
54. Wang, Y.J.; Tan, W.; Liu, C.Y.; Fang, Y.X. Deacidification of Paper in Supercritical Carbon Dioxide (CO<sub>2</sub>SCF) Solvent System with Magnesium Acetate and Calcium Hydroxide. *Adv. Mater. Res.* **2011**, *347–353*, 504–507. [[CrossRef](#)]
55. Tan, W.; Cheng, L.F.; Fang, Y.X. Deacidification of Paper Using Supercritical Carbon Dioxide Containing Calcium Propionate or Magnesium Bicarbonate. *Adv. Mater. Res.* **2013**, *781–784*, 2637–2640. [[CrossRef](#)]
56. Yanjuan, W.; Yanxiong, F.; Wei, T.; Chunying, L. Preservation of Aged Paper Using Borax in Alcohols and the Supercritical Carbon Dioxide System. *J. Cult. Herit.* **2013**, *14*, 16–22. [[CrossRef](#)]
57. Kang, S.M.; Unger, A.; Morrell, J.J. The Effect of Supercritical Carbon Dioxide Extraction on Color Retention and Pesticide Reduction of Wooden Artifacts. *J. Am. Inst. Conserv.* **2004**, *43*, 151–160. [[CrossRef](#)]
58. Tello, H.; Unger, A.; Gockel, F.; Jelen, E. Decontamination of Ethnological Objects with Supercritical Carbon Dioxide. In Proceedings of the ICOM Committee for Conservation 14th Triennial Meeting, The Hague, The Netherlands, 12–16 September 2005; James & James/Earthscan: London, UK, 2005; pp. 110–119.
59. Tello, H.; Unger, A. Liquid and Supercritical Carbon Dioxide as a Cleaning and Decontamination Agent for Ethnographic Materials and Objects. In Proceedings of the Pesticide Mitigation in Museum Collections: Science in Conservation, Washington, DC, USA; Smithsonian Institution Scholarly Press: Washington, DC, USA, 2010; pp. 35–50 (23–24 April 2007).
60. Tuminello, W.H.; Bracci, S.; Piacenti, F. New Developments in Fluorinated Materials for Stone Preservation. *APT Bull. J. Preserv. Technol.* **2002**, *33*, 19–22. [[CrossRef](#)]
61. Balcar, N.; Barabant, G.; Bollard, C.; Kuperholc, S.; Keneghan, B.; Laganà, A.; van Oosten, T.; Segel, K.; Shashoua, Y. Studies in Cleaning Plastics. In *Preservation of Plastic Artefacts in Museum Collections (POPART)*; Lavédrine, B., Fournier, A., Martin, G., Eds.; Comité des Travaux Historiques et Scientifiques (CTHS): Paris, France, 2012; pp. 225–269. Available online: <https://popart-highlights.mnhn.fr/active-conservation-of-plastic-artefacts/studies-in-cleaning-plastics/index.html> (accessed on 6 February 2024).
62. Bartoletti, A.; Soares, I.; Ramos, A.M.; Shashoua, Y.; Quye, A.; Casimiro, T.; Ferreira, J.L. Assessing the Impact and Suitability of Dense Carbon Dioxide as a Green Solvent for the Treatment of PMMA of Historical Value. *Polymers* **2023**, *15*, 566. [[CrossRef](#)]
63. Kazarian, S.G.; Vincent, M.F.; Bright, F.V.; Liotta, C.L.; Eckert, C.A. Specific Intermolecular Interaction of Carbon Dioxide with Polymers. *J. Am. Chem. Soc.* **1996**, *118*, 1729–1736. [[CrossRef](#)]
64. Kazarian, S.G.; Brantley, N.H.; West, B.L.; Vincent, M.F.; Eckert, C.A. In Situ Spectroscopy of Polymers Subjected to Supercritical CO<sub>2</sub>: Plasticization and Dye Impregnation. *Appl. Spectrosc.* **1997**, *51*, 491–494. [[CrossRef](#)]
65. Shieh, Y.-T.; Su, J.-H.; Manivannan, G.; Lee, P.H.C.; Sawan, S.P.; Spall, W.D. Interaction of Supercritical Carbon Dioxide with Polymers. I. Crystalline Polymers. *J. Appl. Polym. Sci.* **1996**, *59*, 695–705. [[CrossRef](#)]
66. Shieh, Y.-T.; Su, J.-H.; Manivannan, G.; Lee, P.H.C.; Sawan, S.P.; Spall, W.D. Interaction of Supercritical Carbon Dioxide with Polymers. II. Amorphous Polymers. *J. Appl. Polym. Sci.* **1996**, *59*, 707–717. [[CrossRef](#)]
67. Alessi, P.; Cortesi, A.; Kikic, I.; Vecchione, F. Plasticization of Polymers with Supercritical Carbon Dioxide: Experimental Determination of Glass-transition Temperatures. *J. Appl. Polym. Sci.* **2003**, *88*, 2189–2193. [[CrossRef](#)]



68. Watanabe, M.; Hashimoto, Y.; Kimura, T.; Kishida, A. Characterization of Engineering Plastics Plasticized Using Supercritical CO<sub>2</sub>. *Polymers* **2020**, *12*, 134. [[CrossRef](#)] [[PubMed](#)]
69. Gong, H.; Zhang, H.; Xu, L.; Li, Y.; Dong, M. Effects of Cosolvent on Dissolution Behaviors of PVAc in Supercritical CO<sub>2</sub>: A Molecular Dynamics Study. *Chem. Eng. Sci.* **2019**, *206*, 22–30. [[CrossRef](#)]
70. Viana, C. Are All Vinyl Paints the Same? The Impact of Paint Formulations on Their Stability and the State of Conservation of Ângelo De Sousa's Paintings. Master's Thesis, NOVA School of Science and Technology, Almada, Portugal, 2022. Available online: <http://hdl.handle.net/10362/141569> (accessed on 6 February 2024).
71. Ferreira, J.L.; Melo, M.J.; Ramos, A.M. Poly(Vinyl Acetate) Paints in Works of Art: A Photochemical Approach. Part 1. *Polym. Degrad. Stab.* **2010**, *95*, 453–461. [[CrossRef](#)]
72. Mahy, M.; Van Eycken, L.; Oosterlinck, A. Evaluation of Uniform Color Spaces Developed after the Adoption of CIELAB and CIELUV. *Color Res. Appl.* **1994**, *19*, 105–121. [[CrossRef](#)]
73. Oleari, C. *Standard Colorimetry: Definitions, Algorithms and Software*; John Wiley & Sons: Hoboken, NJ, USA, 2015.
74. dos Santos, K.A.M.; Suarez, P.A.Z.; Rubim, J.C. Photo-Degradation of Synthetic and Natural Polyisoprenes at Specific UV Radiations. *Polym. Degrad. Stab.* **2005**, *90*, 34–43. [[CrossRef](#)]
75. Xiang, K.; Wang, X.; Huang, G.; Zheng, J.; Huang, J.; Li, G. Thermal Ageing Behavior of Styrene–Butadiene Random Copolymer: A Study on the Ageing Mechanism and Relaxation Properties. *Polym. Degrad. Stab.* **2012**, *97*, 1704–1715. [[CrossRef](#)]
76. Zhang, P.; He, J.; Zhou, X. An FTIR Standard Addition Method for Quantification of Bound Styrene in Its Copolymers. *Polym. Test* **2008**, *27*, 153–157. [[CrossRef](#)]
77. Wei, S.; Pintus, V.; Schreiner, M. Photochemical Degradation Study of Polyvinyl Acetate Paints Used in Artworks by Py–GC/MS. *J. Anal. Appl. Pyrolysis* **2012**, *97*, 158–163. [[CrossRef](#)] [[PubMed](#)]
78. França De Sá, S.; Viana, C.; Ferreira, J.L. Tracing Poly(Vinyl Acetate) Emulsions by Infrared and Raman Spectroscopies: Identification of Spectral Markers. *Polymers* **2021**, *13*, 3609. [[CrossRef](#)] [[PubMed](#)]

**Disclaimer/Publisher's Note:** The statements, opinions and data contained in all publications are solely those of the individual author(s) and contributor(s) and not of MDPI and/or the editor(s). MDPI and/or the editor(s) disclaim responsibility for any injury to people or property resulting from any ideas, methods, instructions or products referred to in the content.